



Contents lists available at ScienceDirect

## Geotextiles and Geomembranes

journal homepage: [www.elsevier.com/locate/geotexmem](http://www.elsevier.com/locate/geotexmem)

# Influence of polymer enhancement on water uptake, retention and barrier performance of geosynthetic clay liners

Zhi Chong Lau<sup>a</sup>, Abdelmalek Bouazza<sup>b,\*</sup>, Will P. Gates<sup>c</sup>

<sup>a</sup> Department of Civil Engineering, 23 College Walk, Monash University, Melbourne, Vic, 3800, Australia

<sup>b</sup> Department of Civil Engineering, 23 College Walk, Monash University, Melbourne, Vic, 3800, Australia

<sup>c</sup> Institute for Frontier Materials, Deakin University, Melbourne, Vic, 3125, Australia

## ARTICLE INFO

## Keywords:

Geosynthetics  
GCLs  
Polymers  
Unsaturated  
Water retention curves

## ABSTRACT

This paper explores the influence of polymer enhancement on water uptake and retention by geosynthetic clay liners (GCLs) across a wide suction range (up to  $10^6$  kPa), including the low suction regime (0.1–10 kPa) typically omitted in past studies. The suction measurement methods used enabled elucidation of water uptake and retention behaviour through the framework of GCL pore structures and their corresponding suction regimes. Polymer enhanced GCLs (PE-GCLs) have high maximum water uptake, and both the water entry and air expulsion values tend to be high. Due to high swelling, the onset of geotextile confinement for PE-GCLs was observed at high suctions. The impact of polymer becomes more apparent when the bentonite achieves a pseudo-two-layer interlayer hydration state at a suction of about 40 MPa (RH = 75%). The hydration mechanism for the polymer fraction in bentonite is unique to the specific polymer type, polymer dosage, and manufacturing process. The water retention behaviour at the low suction range is caused by the in-filling of geotextile pores, bentonite swelling and extrusion, and polymer water adsorption. Insights from this study can form the basis for developing a more suitable bimodal generalised model for fitting the water retention curves of GCLs.

## 1. Introduction

Geosynthetic clay liners (GCLs) are widely used along with geomembranes (GMBs) as part of composite liner systems in various waste containment facilities such as municipal and hazardous solid waste landfills, ponds or surface impoundments, heap leach pads, liquors reservoirs, among many others, to minimise contaminant migration from these facilities (Bouazza, 2002, 2021; Bouazza and Bowders, 2009; Hornsey et al., 2010; Bouazza and Gates, 2014; Rowe, 2014; Mazzieri and Di Emidio et al., 2015; Liu et al., 2015; McWatters et al., 2016; Touze-Foltz et al., 2016; Bouazza et al., 2017b; Gates et al., 2020; Ghavam-Nasiri et al., 2020; Rowe and AbdelRazek, 2021; Li et al., 2021).

An important factor in the long-term hydraulic performance of GCLs is the in-field hydration when placed on a subsoil, driven by differences in suction. As water migrates into the GCL, its moisture content increases concomitantly with a decrease in suction, while the converse transpires in the subsoil. This process continues until the suction between the two materials attains equilibrium. Adequate hydration of the GCL ensures that the bentonite forms a sealing barrier with low hydraulic

conductivity. However, the hydration process is generally not straightforward due to several governing factors, including the subsoil grain size distribution, mineralogy, initial water content and pore water chemistry of the subsoil, environmental and operating conditions of the landfill, bentonite quality and, if present, type of polymer additives (Rayhani et al., 2008, 2011; Anderson et al., 2012; Chevrier et al., 2012; Rowe et al., 2011; Sarabian and Rayhani, 2013; Bradshaw et al., 2013; Barclay and Rayhani, 2013; Bouazza et al., 2017a; Acikel et al., 2018a; Carnero-Guzman et al., 2021; Lau et al., 2022). Furthermore, the contact between GCL and subsoil also dictates whether the transport mode for water transfer is vapour or liquid (Rouf et al., 2016). Nevertheless, the overall impact of these factors on GCL hydration can be assessed within the framework of the fundamental constitutive relationship between suction and water content, which is typically depicted in the form of a water retention curve (WRC).

Measurement of the WRC for GCLs has received increased attention in the past two decades (Barroso et al., 2006; Southen and Rowe, 2007; Abuel-Naga and Bouazza, 2010; Beddoe et al., 2010; Bannour et al., 2014; Acikel et al., 2015, 2018b, 2020, 2022; Bouazza et al., 2017a; Lu et al., 2017, 2018; Ghavam-Nasiri et al., 2019; Yesiller et al., 2019;

\* Corresponding author.

E-mail addresses: [zhi.chong.lau@monash.edu](mailto:zhi.chong.lau@monash.edu) (Z.C. Lau), [malek.bouazza@monash.edu](mailto:malek.bouazza@monash.edu) (A. Bouazza), [will.gates@deakin.edu.au](mailto:will.gates@deakin.edu.au) (W.P. Gates).

<https://doi.org/10.1016/j.geotexmem.2022.02.006>

Received 29 September 2021; Received in revised form 14 February 2022; Accepted 22 February 2022

0266-1144/© 2022 Elsevier Ltd. All rights reserved.

Carnero-Guzman et al., 2019; Tincopa et al., 2020; Yu and El-Zein, 2020; Bouazza and Rouf, 2021; Tincopa and Bouazza, 2021) due to its proven role in understanding the redistribution of moisture between the subsoil and the GCL. Quantifying their WRC across the entire relevant suction range has proven challenging due to the complex nature of GCLs, which consist of materials with vastly contrasting water retention behaviours (Abuel-Naga and Bouazza, 2010; Beddoe et al., 2011; Acikel et al., 2018a; Tincopa et al., 2020; Tincopa and Bouazza, 2021). The hydration process of GCLs is even more complicated with the emergence of polymer modified bentonite for applications where exposure to very high electrolyte concentrations occurs or is expected (Katsumi et al., 2008; Di Emidio et al., 2011, 2015; Scalia and Benson, 2014; Salihoglu et al., 2016; Tian et al., 2016; Mazziere et al., 2017; Scalia et al., 2018). Although their hydraulic conductivity performance has been extensively investigated in recent years (Liu et al., 2012; Bohnhoff and Shackelford, 2014; De Camillis et al., 2016; Fehervari et al., 2016; Ozhan, 2018; Scalia et al., 2014; Tian et al., 2019; Chen et al., 2019), except for Lau et al. (2022), there is a dearth of information in the literature on their hydration and water retention behaviours.

The low suction regime has been typically omitted in previous studies on GCL water retention behaviour due to difficulties in reproducible measurements. Thus, the resulting GCL water retention behaviour is often incomplete and truncated. This paper provides further insight into the bimodal (trimodal if considering the dual-porosity of bentonite) water retention behaviour of polymer enhanced GCLs (PE-GCLs) on the wetting path (i.e., hydration process). This investigation tracks the hydration process of the PE-GCLs through the understanding of pore structures and the fundamental suction regimes governing its water retention behaviour.

## 2. Materials

Five different commercially available needle-punched GCLs were used in the current study. Here, they are referred to as GCL1, GCL2, GCL3, GCL4, and GCL5. GCL1 contained polymer enhanced powdered sodium bentonite. GCL 2 contained non-modified conventional granular sodium bentonite, while GCL3, GCL4, and GCL5 contained polymer enhanced granular sodium bentonite with polymer contents ranging between 3.0 and 9.9% and the same bentonite as GCL2. The GCLs' mass per unit area ( $M_{GCL}$ ) was measured according to ASTM D5993 on a sample size of <24 specimens taken randomly from the GCL rolls. Their representative  $M_{GCL}$  was selected for this study to minimise the effects of mass per unit area variation on the experimental results and was based on the most frequent range (mode) of a histogram data set. The relevant characteristics of the five GCLs are summarised in Table 1.

**Table 1**  
Summary of the general characteristics of GCLs used in this study.

Properties	GCL1	GCL2	GCL3	GCL4	GCL5
Polymer enhancement	Yes	No	Yes	Yes	Yes
Polymer Type	Linear	–	Linear	Crosslinked	Crosslinked
Estimated Polymer Content (%)	1.6	–	3.0 <sup>a</sup>	9.9 <sup>a</sup>	4.4 <sup>a</sup>
Bonding	Needle punched	Needle punched	Needle punched	Needle punched	Needle punched
Thermal treatment	Yes	No	No	No	No
Carrier GTX type	Nonwoven + woven scrim	Nonwoven	Nonwoven + woven composite	Nonwoven	Nonwoven
Cover GTX type	Nonwoven	Nonwoven	Nonwoven	Nonwoven	Nonwoven
Bentonite type	Sodium Powder	Sodium Granular	Sodium Granular	Sodium Granular	Sodium Granular
$M_{GCL}$ Range (Representative $M_{GCL}$ ) (kg/m <sup>2</sup> )	5.52–6.58 (5.90–6.10)	5.83–6.75 (6.40–6.60)	4.85–6.61 (5.30–5.60)	5.04–5.72 (5.20–5.40)	4.89–5.90 (5.20–5.40)
$M_{carrier}$ (kg/m <sup>2</sup> )	0.570	0.200	0.308	0.200	0.200
$M_{cover}$ (kg/m <sup>2</sup> )	0.350	0.200	0.300	0.300	0.200
$M_{bent}$ (kg/m <sup>2</sup> )	4.60–5.66	5.43–6.35	4.24–6.00	4.54–5.22	4.49–5.50
As-received GWC (%)	7.3 ± 0.7	9.2 ± 1.0	6.3 ± 0.3	7.4 ± 0.4	7.9 ± 0.5
Maximum GWC at saturation (%)	186–189	147–155	175–190	218–225	205–223
Initial GCL thickness (mm)	7.6–8.8	8.1–8.7	7.6–8.3	7.5–7.8	7.2–7.6

<sup>a</sup> Estimation does not take into consideration the relative mass loss of the base polymer.

The raw bentonite for GCL1 was enhanced with a proprietary polymer that included polyanionic cellulose (PAC) and anionic acrylic polymer (PAA). The polymer used for GCL3, GCL4, and GCL5 is unknown as it is proprietary information. The polymer contents of the enhanced bentonites were estimated using loss on ignition (LOI) tests (Scalia et al., 2014; Tian et al., 2016, 2019; Chen et al., 2019; Wireko et al., 2020). The LOI of the non-modified bentonite in GCL2 (0.8%) formed the baseline for GCL3, GCL4 and GCL5. The baseline LOI value is attributed to the removal of strongly bound water, calcites and other organic matters associated with the bentonite (Scalia et al., 2014; Tian et al., 2016, 2019). Complete combustion of the polymer additives used in GCL3, GCL4 and GCL5 was assumed to have occurred at 550 °C in this test (Tian et al., 2016, 2019; Chen et al., 2019; Wireko et al., 2020). The pure polymer fraction for GCL1 was provided by the manufacturer; thus, in this case, the relative mass loss of the polymer was taken into consideration.

The term “bentonite” presented in this paper always refers to the bentonite core in the GCL where, if present, the polymer was not separated from the bentonite. The index properties of the polymer enhanced bentonite, extracted from the GCLs, were obtained based on the procedures outlined in ASTM D5890 and ASTM D5891 for comparative purposes only, given that current guidelines indicate these standards do not apply to polymer modified bentonites. The cation exchange capacity (CEC) measurement of the <2 µm fraction was obtained using the barium chloride (BaCl<sub>2</sub>) compulsive exchange method (Sumner and Miller, 1996) with barium (Ba<sup>2+</sup>) analysis by X-ray fluorescence (Norris and Hutton, 1969; Battaglia et al., 2006). This method differs from ASTM D7503 as Ba<sup>2+</sup> is used instead of ammonium (NH<sub>4</sub><sup>+</sup>) as the index ion because (i) Ba<sup>2+</sup> has a higher affinity for the exchange complex than NH<sub>4</sub><sup>+</sup> and (ii) Ba<sup>2+</sup> very rarely naturally occupies the exchange complex of smectites, whereas NH<sub>4</sub><sup>+</sup> can and does (e.g. Ernstsen et al., 1998). Therefore, much smaller sample sizes and lower reactant concentrations can be used because the analysis is conducted directly on a dried filter-deposited powdered sample. The mineralogical composition of the bulk bentonite was determined using quantitative X-ray diffraction (XRD) analysis. The bentonite's geotechnical properties and physical and mineralogical characteristics are summarised in Table 2.

## 3. Experimental methods

Multiple measurement methods were employed to cover the wide suction range of bentonite and establish the water retention curve on the wetting path of the GCL. The following section presents the techniques used in the current investigation.

**Table 2**  
Properties of the bentonite component of the GCLs.

Parameter	GCL1	GCL2	GCL3	GCL4	GCL5
Swell index (mL/2 g)	33.1 ± 0.6	25.7 ± 0.7	36.3 ± 0.7	57.6 ± 6.6	42.3 ± 1.7
	13.8 ± 0.2	12.4 ± 0.1	5.9 ± 0.1	8.7 ± 1.4	9.3 ± 0.2
Fluid loss (mL)	85	76	78	79	84
Cation exchange capacity (cmol/kg)					
<b>Particle Size</b>					
D <sub>10</sub> (mm)	0.007	0.65	0.45	0.36	0.10
D <sub>30</sub> (mm)	0.018	0.90	0.69	0.66	0.19
D <sub>60</sub> (mm)	0.042	1.25	1.00	1.00	0.31
Coefficient of uniformity, C <sub>u</sub>	5.88	1.92	2.22	2.78	3.10
Coefficient of curvature, C <sub>c</sub>	1.10	1.00	1.06	1.21	1.10
<b>Mineralogical Composition</b>					
Montmorillonite (wt%)	74	81	80	80	82
Cristobalite (wt%)	8	12	12	12	12
Quartz (wt%)	12	1	1	1	1
Albite/Anorthite (wt%)	4	4	4	4	3
Calcite (wt%)	<1	<1	1	1	<1
Kaolin (wt%)	1	–	–	–	–
Anatase (wt%)	<1	–	–	–	–
Zeolite (wt%)	1	1	1	1	1
Mica (wt%)	–	1	1	1	1
Gypsum (wt%)	–	<1	<1	<1	<1

### 3.1. Vapour sorption method

A Vapour Sorption Analyzer (VSA) (METTER Group, Pullman, WA) was used to measure the water retention over the range of  $5 \times 10^3$ – $5 \times 10^5$  kPa suction. The measurements were conducted on the bentonite component of the GCL only due to the chamber size limitation of the equipment. Furthermore, previous studies have proven the dominance of the bentonite in controlling the behaviour of GCLs in the high suction range (Beddoe et al., 2011; Rouf et al., 2016; Acikel et al., 2018a; Tin-copa et al., 2020; Carnero-Guzman et al., 2019, 2021; Bouazza and Rouf, 2021). The vapour-equilibrium process is diffusion-limited and can take considerable time, depending on the method used, especially for high relative humidity (RH) (>95%, Rouf et al., 2016) or low RH (<15%, Gates et al., 2017). Thus, measurements using the VSA were obtained with the Dynamic Vapour Sorption (DVS) method, which produces equilibrium isotherms, albeit taking a longer time. In this method, extracted bentonite was placed in a closed chamber and kept at a temperature of  $20 \text{ }^\circ\text{C} \pm 0.2 \text{ }^\circ\text{C}$ . Its mass was continuously measured as it underwent hydration through vapour adsorption under various pre-set RH. The wetting cycle started from 5% RH to 95% RH at 10% step increments. The chamber's humidity was controlled by drying the air using desiccant tubes or wetting it using vapour saturated air from its internal water reservoir. The specimen was held at the controlled pre-set humidity until the mass change over time was <0.05%/hr over multiple measurements, typically taken every 5–6 min, when it was deemed to have reached equilibrium. The equilibrium mass was recorded with a corresponding suction value. The instrument then proceeded to the next step at a higher RH by repeating the above process.

### 3.2. Super-saturated salt solution controlled free swell method

A vapour equilibrium technique (VET) using super-saturated salt solutions based on the methodology presented by Rouf et al. (2014, 2016) was used to obtain the GCL water retention properties over suctions ranging from 2000 kPa to  $10^5$  kPa. These suction measurements were also used to validate the data obtained using the VSA. GCL specimens (30 mm in diameter) were prepared based on their representative mass per unit area. Once cut, they were sealed around the edges using silicone gel to minimise bentonite loss during handling. The specimens

were placed on a wire mesh platform in sealed humidity-controlled containers that contained different salt solutions targeting various RH values. The super-saturated salt solutions were prepared following ASTM E104 and included the following:  $\text{K}_2\text{CO}_3$  (43.2% RH), NaBr (57.6% RH), KI (68.9% RH), NaCl (75.3% RH), KCl (84.2% RH),  $\text{K}_2\text{NO}_3$  (93.7% RH),  $\text{K}_2\text{SO}_4$  (97.3% RH). They were used to generate and maintain a stable RH environment in the container during the experiment. The experiments were conducted in a climatic chamber at  $20 \text{ }^\circ\text{C} \pm 0.2 \text{ }^\circ\text{C}$ . The specimen mass measurements were periodically taken until mass equilibrium was deemed to have been attained (i.e. consecutive measurements of <1% mass change). This process allowed the calculation of the GWC for the corresponding suction.

### 3.3. Chilled mirror hygrometer method

A WP4C dew-point potentiometer was chosen for GCL intermediate suction range measurements. This method overlaps with the suction range covered by the VSA and the VET but attains lower suctions. While the WP4C can be used to measure from 0 to  $3 \times 10^5$  kPa, the accuracy of the measurements decreases significantly below 5000 kPa, where the accuracy is  $\pm 50$  kPa ( $\pm 1\%$ ). Thus, measurements using the WP4C were limited to around 1000 kPa, with a measurement accuracy of  $\pm 5\%$ . All the WP4 tests were conducted at a temperature of  $20 \text{ }^\circ\text{C}$ . Measurements at higher suction using this method were also used to validate VSA and VET data. The chilled mirror hygrometer method measures the total suction via the dew point of the enclosed chamber environment by assuming vapour phase equilibrium between the GCL sample and the air in the measurement chamber. The two primary considerations that must be excogitated when taking measurements of the GCL are the effects of the conditioning time and the testing time (Acikel et al., 2018b). Thus, this test was undertaken following the procedures outlined in Acikel et al. (2018b). The GCL specimens were placed in metal containers and hydrated to various target gravimetric water contents. The containers were sealed and given a conditioning time of one week to ensure moisture homogenisation in the GCL specimen. Before taking measurements, the specimens were left undisturbed in the WP4C overnight to minimise testing time dependency. Multiple measurements of each specimen were taken, and the average suction measurement was taken to be the representative total suction of each specimen.

### 3.4. Initial wet contact filter paper test

Experimental measurements for GCLs at very low suctions are scarce due to the difficulty in achieving accurate measurements. Conventional filter paper methods, as outlined in ASTM D5298, were shown by Acikel (2016) to yield unrealistic suction values (i.e., matric suction > total suction) for GCLs and require a longer testing time than the seven days recommended due to the bentonite component necessitating a lengthier moisture homogenisation process. The initial wet contact filter paper test (IWCFT) was deemed most appropriate for the wetting path where matric suction measurements can be made accurately up to 146 kPa as reported in Acikel et al. (2015). The main issue with longer pre-conditioning and testing times is that microbial contamination on the filter papers may taint measurements made during the experiment; thus, sterilisation, conditioning and test duration protocols, appropriate for GCLs, were used following Acikel et al. (2015). GCL specimens (50 mm in diameter) were cut, sealed around the edges using polyurethane sealant, and then hydrated to various target gravimetric water contents using sterilised distilled water. The specimens were wrapped in sealable bags and stored in an insulated box under two kPa confining pressure at a temperature of  $21 \text{ }^\circ\text{C}$  for six weeks to allow moisture homogenisation. Whatman no. 42 filter papers were sterilised using 2% formaldehyde (ASTM D5298), and subsequently oven-dried. The GCL specimen was sandwiched between two sterilised filter paper stacks (each consisting of two 50 mm diameter cover filter paper with a 42.5 mm diameter sensor filter paper in between). For the IWCFT, the sensor filter paper was first

soaked in sterilised distilled water for 1 h, and a 2 kPa pressure was applied to ensure good capillary contact between the filter paper stacks and the GCL. The test specimens were sealed in new zip-close plastic bags and stored for a further four weeks to ensure that equilibrium was achieved between the sensor filter paper and the GCL. Subsequently, both the water contents of the filter paper and the GCL were measured. The equilibrium suction value was calculated from the filter paper water content using the bilinear equation proposed by Leong et al. (2002), as shown in Equations (1) and (2) below, which is the most accurate method of calibration for the filter paper type used (Acikel et al., 2011). It should be noted that the data points used for calibration did not include data points with suction <10 kPa. However, an assumption is made that the wetting behaviour of the filter paper beyond its water entry value ( $w_f \geq 47$ ) would trend similarly at suctions <10 kPa.

$$\log \psi = 2.909 - 0.0229 \times w_f \quad w_f \geq 47 \quad (1)$$

$$\log \psi = 4.945 - 0.0673 \times w_f \quad w_f < 47 \quad (2)$$

where the  $\psi$  is the matric suction and  $w_f$  is the filter paper water content in percentage.

## 4. Results and discussions

### 4.1. Water retention regimes and suction mechanisms

The water retention curves (WRC) for each of the GCLs on their wetting paths, with each WRC built from four different, largely overlapping measurement methods, are shown in Fig. 1. The high suction range (>5000 kPa) is populated using the data from VSA and, for GCL1, this includes data from VET. The intermediate region (primarily 800 – 10<sup>4</sup> kPa) was populated using the WP4C data, while the low suction region (<146 kPa) was constructed using the IW-CFPT data. It can be observed that at very low suction (very wet specimens), the GCLs exhibit a bimodal characteristic rather than the typical unimodal, sigmoidal curve reported by several researchers (Barroso et al., 2006; Southern and Rowe, 2007; Beddoe et al., 2011; Bannour et al., 2014; Acikel et al., 2018a; Ghavam-Nasiri et al., 2019; Tincopa et al., 2020; Tincopa and

Bouazza, 2021). Most of these studies did not extend their suction measurements below 10 kPa, likely because the behaviour of the bentonite component was adequately captured at suctions higher than 10 kPa, which masked the bimodal behaviour of the GCL. While a small gap in the data exists between ≈50 and ≈1000 kPa, the WRC depicted in Fig. 1 indicates how all these different methods can be used to access the full suction range for various GCLs, including PE-GCLs.

Polymer type, polymer loading, and GCL structure play a role in the bentonite swelling and, consequently, the amount of water uptake, especially at the low suction region. When comparing the WRC of the various GCLs gravimetrically, as shown in Fig. 2a, it can be observed that the saturated gravimetric water content varies widely. GCLs with higher polymer loading tend to achieve a higher maximum gravimetric water content than their equivalent non-modified product: e.g.  $w = 183\%$  for GCL3,  $w = 223\%$  for GCL4, and  $w = 214\%$  for GCL5 compared to  $w = 151\%$  for GCL2. Thus, gravimetric WRCs (G-WRC) are dependent on the GCL product.

The WRC was quantified volumetrically to account for volume changes in the GCL during hydration, as shown in Fig. 2b. It can be observed that while the GWC of the various GCLs varies widely from 123% to 235% (i.e. at 0.1 kPa suction), this variation becomes significantly less in terms of volumetric WRC (V-WRC), where the VWC was within the range of 0.66–0.80. Furthermore, the V-WRC also reveals that the water retention behaviour of the GCLs at suctions higher than 1000 kPa was the same regardless of the different types of GCLs. Generally, the GCLs follow a similar wetting path and hydrate up to a VWC of 0.55 (0.52–0.57 based on Fig. 2b), coinciding with the air expulsion values (AEV). At lower suctions (0.01 kPa–146 kPa), V-WRCs (0.50–0.80) respond within a significantly narrower range compared to the gravimetric WRC (100%–235%). This observation indicates that, as expected, the bulk of the volume change occurs in the low suction region, where increased bentonite swelling increases the GCL volume. Because of this, the bimodal shape of the GCL G-WRCs observed is not as apparent in the V-WRC, particularly for the PE-GCLs, which exhibited higher swelling behaviour.

The WRC of a material is commonly associated with its pore size distribution, pore structure, chemical and mineralogical composition of

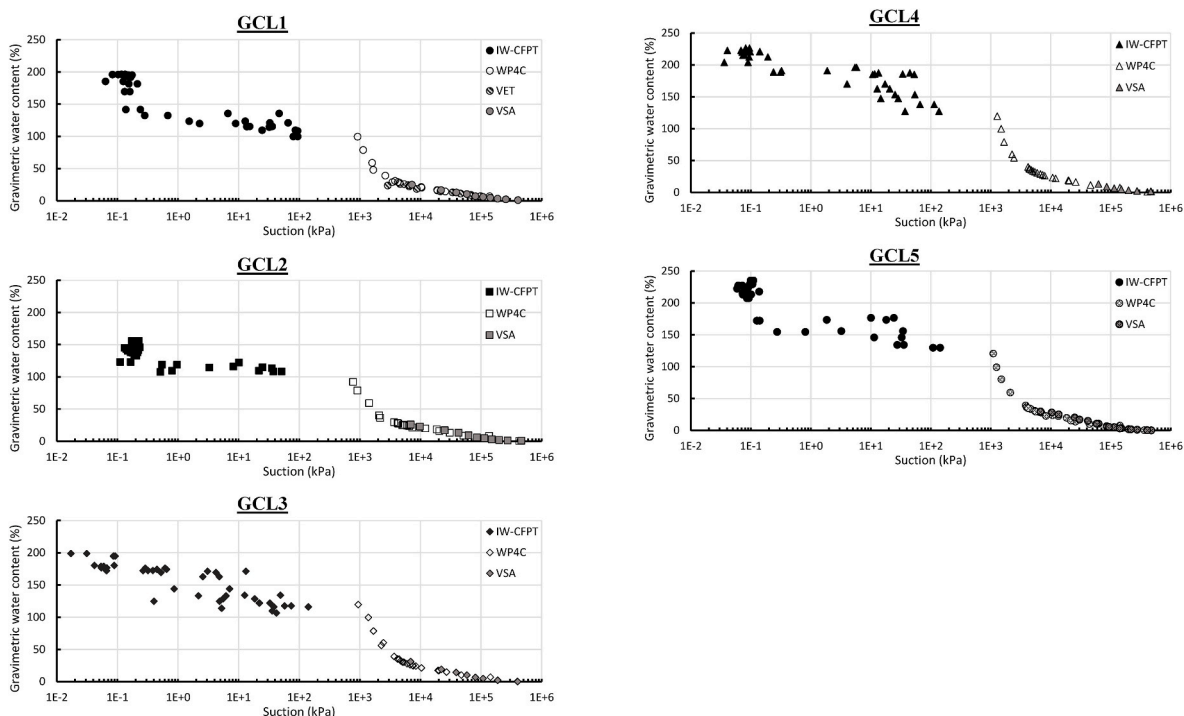


Fig. 1. Water retention curve (WRC) of the respective GCLs.

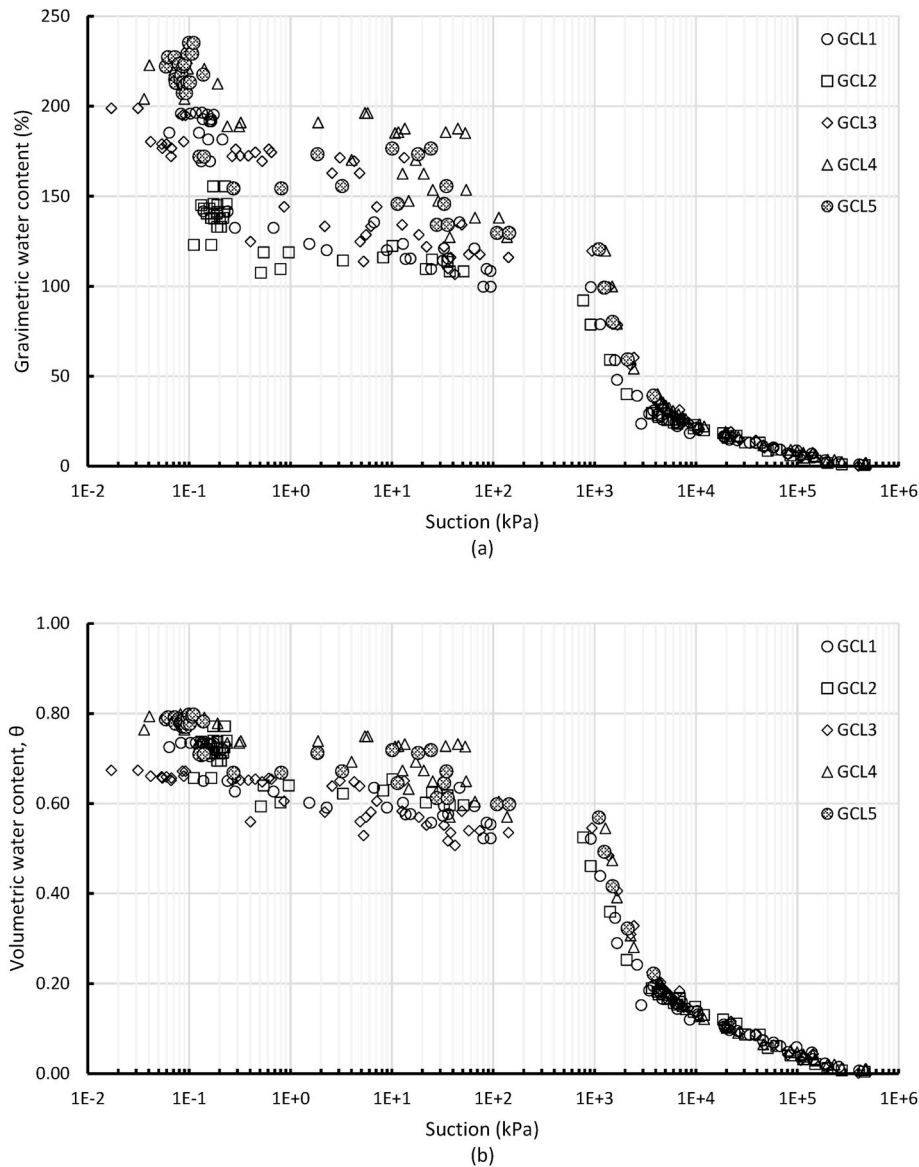


Fig. 2. The overall combined water retention curve (WRC) of the GCLs in terms of (a) gravimetric water content, (b) volumetric water content.

materials like bentonite (Likos et al., 2010; Lu, 2016). The WRCs described in Fig. 2 indicate the presence of at least four different slopes: between the suction ranges of 0.1–0.3 kPa, 0.3–1000 kPa, 1000–4000 kPa, and >4000 kPa, where there is generally a small increase in water content corresponding to a large decrease in suction and then a large increase in water content over a small drop in suction. Such a response is indicative of the presence of multiple segregated pore sizes in the material corresponding to a bimodal water retention behaviour (Burger and Shackelford, 2001; Zhang and Chen, 2005; Satyanaga et al., 2013). This observation aligns with the composite nature of GCL, where its constituent elements have vastly different pore sizes. The geotextile component typically has an apparent opening size of 0.1–0.2 mm (Bouazza et al., 2006a; 2006b), while the granular bentonite has an inter-grain pore size of 15–30  $\mu\text{m}$  (Seiphoori et al., 2016) and approximately 0.1  $\mu\text{m}$  for powder bentonite (Liu et al., 2020). Furthermore, bentonite itself has often been characterised using a bimodal pore structure by many researchers regardless of the bentonite form (Gens and Alonso, 1992; Alonso et al., 1999; Sanchez et al., 2006, 2016; Delage, 2007; Villar and Lloret, 2008; Romero et al., 2011; Seiphoori et al., 2014; Navarro et al., 2015; Cui, 2017; Acikel et al., 2018a). The dual-porosity of bentonite is delineated where the pores between

bentonite aggregates (inter-aggregate pores) are considered macropores and the pores within the bentonite matrix (i.e. intra-aggregate pores and smaller interlayer pores of the clay mineral component) are deemed to be micropores. It should be noted that the intra-aggregate and inter-particle pores, usually between 2 and 50 nm in diameter, are also referred to in the literature as bentonite mesopores (Villar et al., 2012). However, within the context of bentonite swelling in GCLs, intra-aggregate pores can also be the same size as interlayer pores (micropores: <5 nm, Gates et al., 2021). Therefore, when viewed in its entirety, taking into consideration both the geotextile and bentonite pores, the GCL is considered to have a trimodal pore structure (Acikel et al., 2018a, 2020; Gates et al., 2018).

This fundamental understanding of GCLs pore structures provides a frame of reference when examining the suction mechanism that dictates their water retention behaviour. A conceptual model of the GCL water retention curve is illustrated in Fig. 3, along with the corresponding suction regime and pore structures. It should be noted that the polymer bentonite interaction shown in the conceptual model is reflective of GCL1 only, as the composition of the polymers in GCL3, GCL4, and GCL5 is unknown (proprietary information). During hydration, water transported through the pores exists as capillary water and adsorbed water

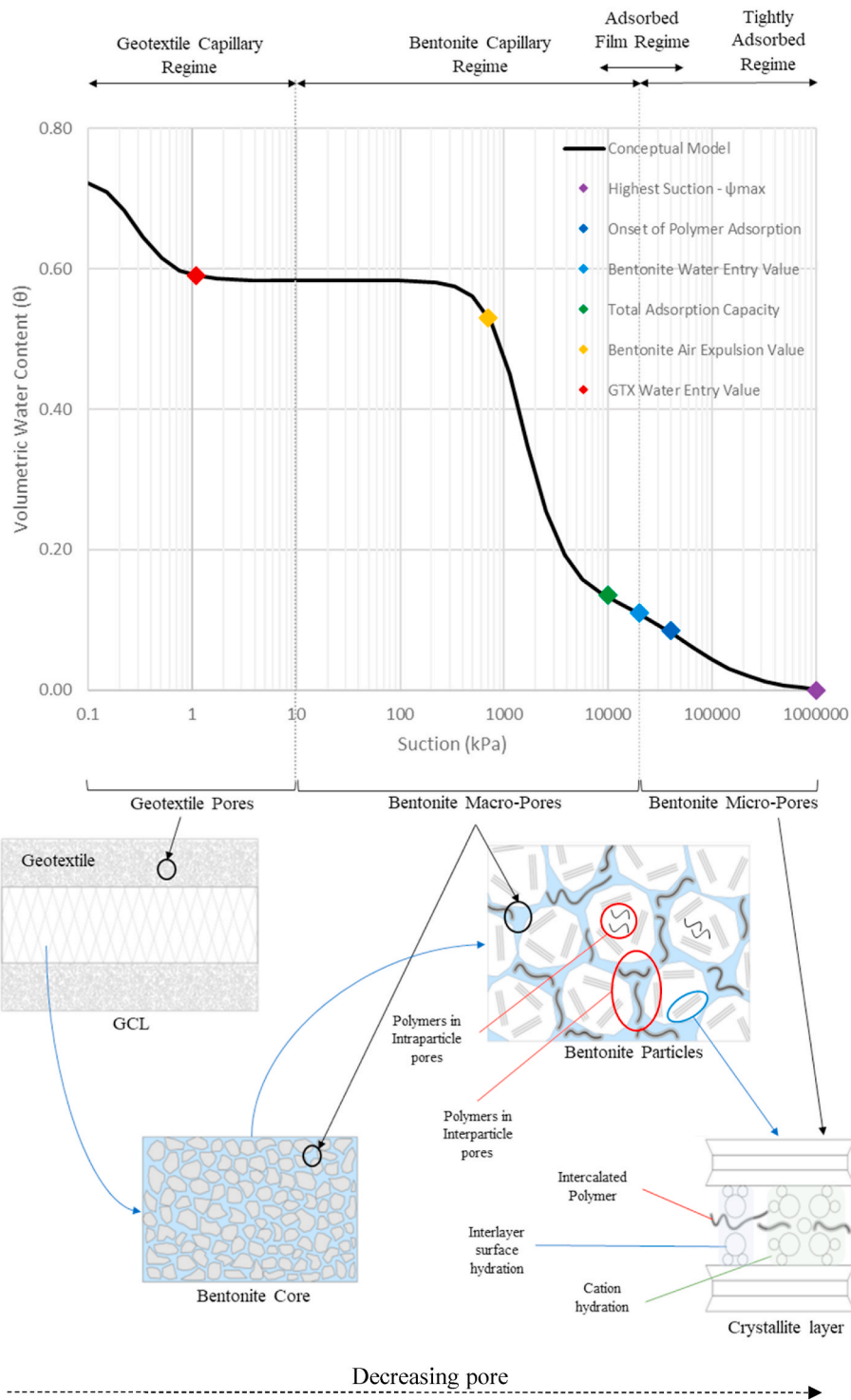


Fig. 3. Conceptual model of an idealised GCL water retention curve with the corresponding suction regime categories and examples of pore structures.

(Tuller et al., 1999; Frydman and Baker, 2009; Lu, 2016). Under a typical wetting process scenario, the GCL starts from a relatively dry state (~10% GWC). At various points in its transition to a fully saturated state, the pore water in the GCL is held in an unsaturated state under different suction regimes. The important suction regimes for GCLs are the tightly adsorbed, adsorbed film and capillary regimes (Fig. 3) (McQueen and Miller, 1974; Lu and Khorshidi, 2015). The tightly adsorbed water discussed in this paper is often referred to in the clay minerals literature as tightly bound water (TBW). By extrapolation, other adsorbed water relates to weakly bound water (WBW)

(Kuligiewicz and Derkowski, 2017). While this framework would adequately capture the water retention behaviour of the GCL's bentonite component, it is proposed that for GCLs, further considerations should be placed on the capillary regime of the geotextile component and, if present, the adsorbed water of any polymer fraction.

#### 4.2. Bentonite micropores (adsorption water)

At its as-received water content, the GCL is relatively dry and has low matric potential or high suction, where it is assumed that there is no

water in the capillary pores. Thus, indirect measurement techniques using the VSA, VET and WP4C were employed to measure its total suction. The high suction range behaviour of GCLs have been shown in previous studies to be governed by the bentonite fraction. Thus, to support this assertion, comparisons between suction measurements of the GCLs and their bentonite component were conducted, as shown in Fig. 4. It should be noted that the measurements for the bentonite using WP4C have an accuracy of  $\pm 50$  kPa.

Fig. 4 indicates that the relationship between GWC and suction for both the GCL and its bentonite follows a similar wetting path in the intermediate to high suction range (at suctions larger than  $\sim 1000$ – $5000$  kPa). However, the bentonite WRC is slightly higher than GCL WRC. The differences between the GCL and bentonite WRCs can be attributed to the GWC of the GCLs also incorporating the mass of their geotextile components. Thus, the GCL water contents were normalised to their proportional mass of bentonite ( $M_{bent}$ ) from Table 1, as shown in Fig. 4 using the cross marked data points to allow for a more valid direct comparison to their bentonite-only WRC (Carnero-Guzman et al., 2019). The conversion was estimated using the following equation:

$$W_{norm} = \frac{W_{GCL}M_{GCL}}{M_{bent}} \quad (3)$$

where  $W_{norm}$  is the normalised GCL GWC considering only its bentonite component,  $W_{GCL}$  is the measured experimental GCL GWC,  $M_{GCL}$  is the mass per unit area of the GCL, and  $M_{bent}$  is the mass per unit area of the bentonite in the GCL (calculated by deducting the mass per unit area of the geotextile components,  $M_{bent} = M_{GCL} - M_{carrier} - M_{cover}$ ). The normalised GWC of the GCL at the high suction range ( $>1000$  kPa) showed better agreement with the measured bentonite WRC data, highlighting

that the bentonite core almost entirely controls the water retention behaviour of the GCL at these suctions. The only exception to this observation is GCL4, where GCL4's bentonite-only WRC is higher around its water entry value (WEV) compared to its normalised GCL WRC. It is inferred herein that due to GCL4's high polymer loading and high swelling behaviours, the onset of geotextile confinement on the polymer modified bentonite core probably occurred in this suction regime.

Overall, this result is consistent with the findings of Beddoe et al. (2011) and Carnero-Guzman et al. (2019), where comparisons made with other published data on the wetting path showed the dominance of the bentonite component at suctions  $\gg 10$  MPa. These findings are unsurprising as the exchange cations in montmorillonite clay minerals (which controls the water sorption regime above  $\sim 10^4$  kPa) have high hydrating energies allowing the bentonite to absorb and retain water at high suction (Bordallo et al., 2008; Gates et al., 2012, 2017). The positively charged exchangeable cations in the mineral interlayers attract dipolar water molecules, with subsequent shells having weaker bonds. Since the Coulomb force is responsible for this interaction is within the atomic scale, it operates within the suction range in the order of a hundred thousand of kPa (Lu, 2016). Furthermore, hydration of the interlayer and intra-particle pore surfaces also accounts for the adsorbed water for suctions above 3000 kPa. Although it is likely that the surface hydration mechanism only occurs at suctions lower than the cation hydration mechanism because the attractive van der Waals forces between the mineral surface and water molecules are orders of magnitude smaller (Israelachvili, 2011). Other interactions leading to surface hydration occur through hydrogen bonding (H-bonding) attraction of water to negatively charged mineral surface (Likos et al., 2010).

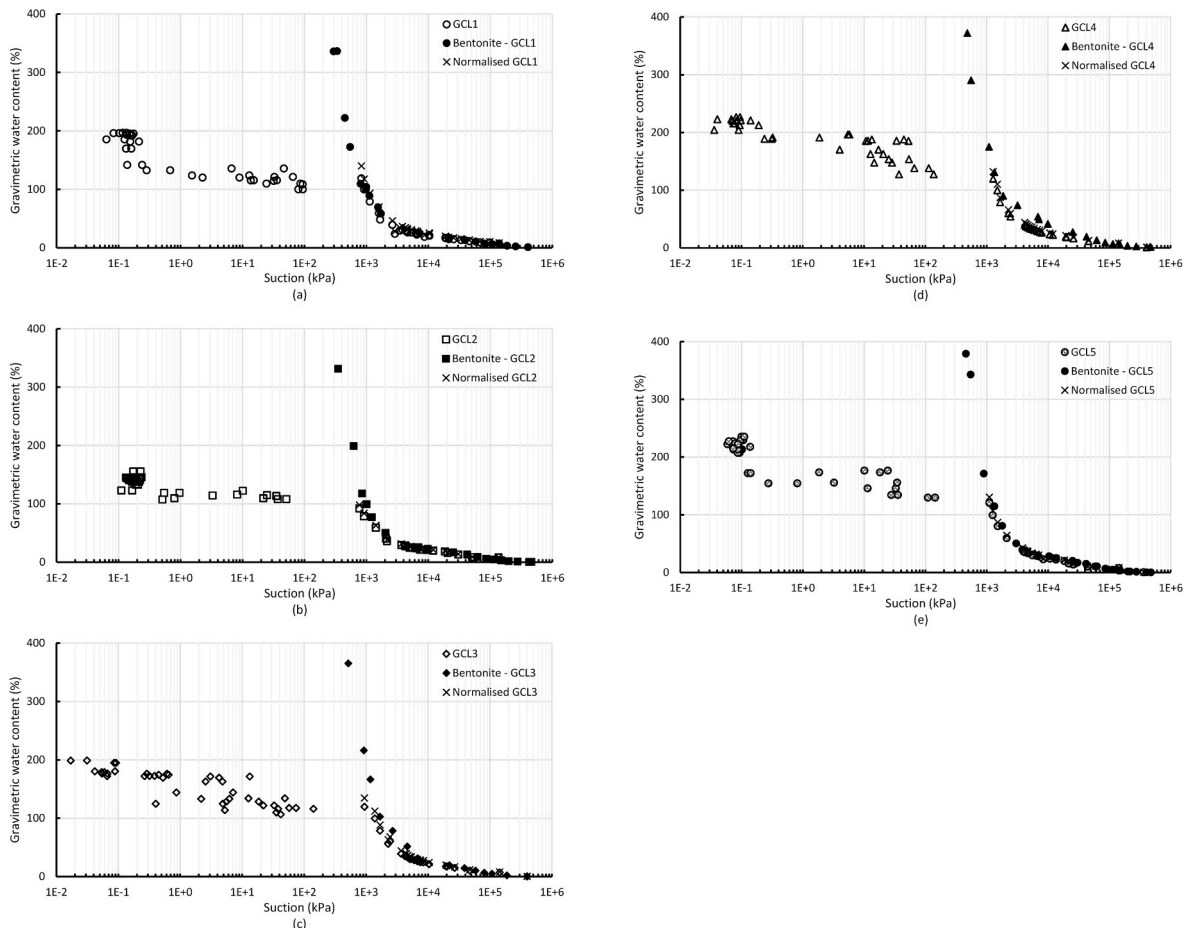


Fig. 4. Comparison between the water retention behaviour of the GCLs and their bentonite fraction.

A conceptual description of the water adsorption process in GCLs will start from bentonite micropores being in an unsaturated state until capillarity forms in the bentonite macropores. Since capillary connections have not formed, the hydration process occurs through vapour phase transport. As the initially dry material begins to wet, the smectite forms a metastable pseudo monolayer hydrated (1LW) state with a  $\approx 1.2$ – $1.3$  nm basal spacing (Laird, 1996). Subsequently, as observed in Fig. 4, as the suction decreases, the gravimetric water content increases, which corresponds with more discrete layers of water molecules, as many as four discrete hydration layers (Mooney et al., 1952; Norrish, 1954), forming around the exchangeable cations and an increased interlayer surface hydration coverage (Khorshidi et al., 2017). This process underpins the crystalline swelling of the bentonite, where the introduction of water into the interlayer space causes partial disassociation between the unit layers held together by weak electrostatic bonds.

The water around the exchangeable cations and the interlayer surfaces of bentonite make up the tightly adsorbed water regime. The upper bound of this regime is the highest suction value of the bentonite (Jensen et al., 2015; Lu and Khorshidi, 2015), and the lower bound of this regime is demarcated by the suction value corresponding to the amount of strongly adsorbed water in the micropores, which ranges between 25% and 40% GWC for different bentonites (Gates et al., 2017,2021; Carnero-Guzman et al., 2019, 2021). Both boundaries are a function of bentonite mineralogy and cation type and the resulting microstructural changes induced by changing hydration conditions. Although the suction mechanism for capillary water and adsorption water is distinct, there is an overlap where both mechanisms operate within the same suction range. This intermediary water retention regime is considered to be the adsorbed film regime. Here, the water adsorbed through surface hydration forms a continuous film on particle surfaces and, closer to the lower limit of the suction range, capillary water forms within corners of contact between particles (Tuller et al., 1999). The total adsorption water in the system is considered to be the lower boundary of this regime and is a unique physical parameter in models proposed by Lu (2016). As with the highest suction parameter, the total adsorption capacity of the bentonite is also dependent on its mineralogy (Tuller and Or, 2005; Revil and Lu, 2013; Rouf et al., 2016).

#### 4.3. Bentonite mesopores and macropores (capillary water)

As described in the preceding section, the initial hydration process of the exchangeable cation results in crystalline swelling, where an increased separation between the crystallites and separation of quasi-crystals forming intra-particle pores occurs (Acikel et al., 2018b). The decrease in crystallite layer number per particle (separation of quasi-crystals) was reported to be most evident over the 2800–6900 kPa suction range (Saiyouri et al., 2004). Both interlayer and intra-particle pores bridge the micropore-mesopore boundary. Whilst the exchangeable cations are restrained within the interlayer space, the attractive electrostatic forces of the smectite surface no longer dominate their interactions. Thus, the interlayer water is deemed a region with higher ionic strength due to the cations compared to the pore water in the mesopores. The transition beyond crystalline swelling begins in the adsorbed film regime, where adsorbed film forms around the partially swollen bentonite quasi-crystals and particles (in the mesopores). The resulting osmotic suction exerted between the interlayer water and the capillary pore water in the mesoporous intra- and inter-particle pore space initiates water movement into the microporous interlayer space, where the clay unit layers continue to disassociate as the bentonite enters a gel phase (Likos et al., 2010). This phenomenon generally initiates at clay domains with smaller pore sizes, where, with decreased suction, a meniscus develops in the pores (starting at intra-particle pore surface contacts) that gradually forms capillary connections and induces the movement of capillary water into these pores. Subsequently, as the water in the system reaches its adsorption capacity, capillary water becomes the main contributor of water retained in the intermediate

suction range (less than 2–5 MPa, see Table 3). This transition is typically demarcated by the water entry value (WEV) of the GCL; a point that indicates the mean water entry suction value at which capillary connections of the residual water (residing in micropores of the interlayer and intra-particle pores) form between particles in the bentonite mesopores and macropores as described above (Fredlund et al., 2012; Acikel et al., 2018b). Therefore, this regime initiates when capillarity gradually establishes between the clay particles. Nonetheless, it should be noted that the capillary action in the mesopores does not restrict the osmotic swelling regime; in reality, the osmotic suction regime initiates in the bentonite around the pseudo 2- to 3-layer hydrate state as long as there is access to water for this interaction. This is typically associated with the osmotic (or bulk) swelling regime of the bentonite.

In the intermediate suction range, the meso- and macro-pores dictate the water sorption behaviour of the GCL through capillary action (Gates et al. 2021). For GCLs in general, the meso- and macro-pore size boundary depends on the bentonite form, i.e., granular or powder, presence of disturbances by needle punching and rolling. The white arrows in Fig. 5 indicate capillary water in the inter-particle pores, which contributes to the bentonite's osmotic (bulk) swelling and increases bentonite interlayer volume. As the bentonite core in the GCL is confined by the interlocking geotextile fibres, swelling of smectite interlayers partially fills up the interparticle pores to offset the increased volume (Likos and Lu, 2006), gradually shifting the pore size distribution of the bentonite clay domains to sub-micron sizes (Acikel et al. 2018a). The partially hydrated bentonite can also intermix/incorporate into the geotextile pores within the thermal joins of the needle punched fibre bundles (Gates et al., 2018). The needle-punched fibre bundles, indicated by the white rectangles, were considered to be important transits in the hydration process of the bentonite core, where water can move directly into the macropores. Furthermore, largely isolated macropores ("roll pores") associated with non-destructive dry-shearing from the rolling/unrolling action during the manufacturing process are also interspersed within the GCL bentonite matrix as shown by Gates et al. (2018) using micro X-ray computed tomography (XCT). These "roll pores" are indicated by the white circles in the high resolution (7  $\mu$ m pixel resolution) XCT image presented in Fig. 5 and are a few orders of magnitudes larger than the mesopores. The bentonite surrounding these pores was better hydrated, indicating that these pores probably played a substantial role in the further hydration of the GCL bentonite core (i.e., acted as a water source for bentonite osmotic swelling).

If the bentonite were to swell freely, it is capable of large volume changes and attracting significant amounts of water where the osmotic swelling leads to complete disassociation of the quasi-crystal in a dispersed phase. However, in GCL applications, the geotextile and the fibres encapsulating the bentonite, in addition to any overburden stress, exert a confining stress on the swelling bentonite. This restricts the bentonite volume change, and consequently, the amount of water the bentonite effectively absorbs. Thus, the GCL behaviour here closely relates to the GCL's peel strength, where higher peel strength provides a higher degree of confinement. This phenomenon is observed in the WRC of GCLs in the capillary zone, where it diverges from the WRC of their extracted bentonite around 1 MPa (Fig. 4), coinciding with their air expulsion values (AEV) shown in Fig. 4. Thus, as air is expelled from the GCL pores due to bentonite swelling, the geotextile fibres are activated, and the imposed confinement restricts swelling. An exception is GCL4, where the WRC of its extracted bentonite component separates from its GCL WRC at suctions near 10 MPa, perhaps due to its extremely high

**Table 3**

Summary of the AEV and WEV values of the GCLs presented in Fig. 6. See Table 1 for polymer contents of the various GCLs.

	GCL1	GCL2	GCL3	GCL4	GCL5
Air Expulsion Value, AEV (kPa)	800	550	900	1200	950
Water Entry Value, WEV (kPa)	3000	2600	5000	3300	3200

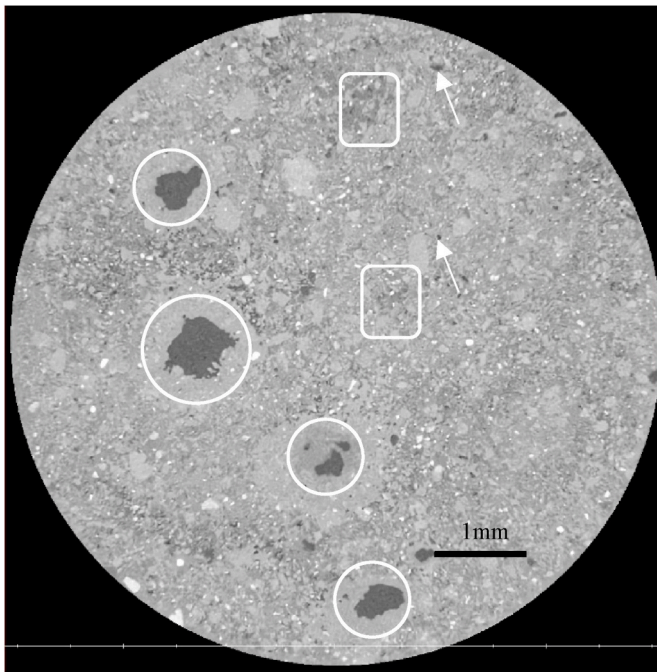


Fig. 5. High resolution micro XCT image showing the longitudinal cross-section of the partially hydrated bentonite (Gates et al., 2018).

swelling capacity (Swell Index = 55.8 mL/2 g), so the onset of geotextile fibre activation begins at higher suctions. Adequate confinement provided by either the vertical stress or fibres is essential to ensure optimal hydraulic performance by the GCL (Abuel Naga and Bouazza, 2013; Rowe, 2013). Under confinement, the bentonite fabric structure changed because quasi-crystals rearrange and fill in void spaces, resulting in a lower void ratio and reduction in hydraulic conductivity due to the increased tortuosity of flow paths (Gates et al., 2009).

The properties typically used to define the starting point of the capillary regime are the points for cavitation suction of the pore water or the residual capillary suction obtained from the water retention curve (Fredlund and Xing, 1994; Or and Tuller, 2002; Frydman and Baker, 2009). While an area of ongoing research, it is generally understood that cavitation occurs gradually over a range of suctions and can be best described using a distribution function (Herbert et al., 2006; Lu, 2016). Most studies on water cavitation in soil mechanics were investigated under desorption conditions as the results were more reproducible. Nonetheless, it can be inferred for the wetting path that the onset of capillary connection would only develop at a suction value less than the cavitation point and would occur as a gradual process. Thus, the corresponding key characteristic that can be obtained from the WRC to delineate the capillary regime and adsorption regime is the water entry value (WEV) (Yang et al., 2004; Acikel et al., 2018a). The water entry value (WEV) is taken to be the suction value at the point of intersection between the tangent line of the capillary regime slope and the straight line approximating the high suction adsorption regime (Fig. 6). This point indicates the mean suction value at which capillary connections form between particles in the bentonite macropores that enable water entry. Moving along the wetting path of the WRC, the bentonite swells as more water migrates into the GCL and air is expelled from the pores until eventually, the bentonite in the GCL becomes fully saturated. The suction at which saturation occurs is defined by the air expulsion value (AEV) on the WRC wetting path as labelled in Fig. 6, similar to the air entry values obtained on the drying path. This point indicates the region in which the bentonite transitions from an unsaturated to a saturated state (Pasha et al., 2017).

The intermediate suction range of the GCL WRCs measured in this study and their corresponding AEV and WEV are illustrated in Fig. 6 and

summarised in Table 3. The results show that GCLs with higher polymer loading like GCL3, GCL4, and GCL5 tend to have higher WEV and AEV than their unmodified counterpart, GCL2. This suggests that the increased water uptake by the polymer modified bentonite has led to the onset of water entry in bentonite capillary pores at higher suctions. Similarly, the air voids in the bentonite are also being expelled at higher suctions. An interesting feature of the WRCs depicted in Fig. 6 is that the shape of the curve near the WEV transition is more curvilinear for the GCLs with higher polymer loading. For example, GCL2 has a distinct inflection point, whereas the others reveal smoother responses of VWC with suction ( $GCL1 < GCL3 < GCL5 < GCL4$ ). A plausible explanation is that because the polymer adsorption sites become active around 40 MPa (see Section 4.5), more water is attracted into the bentonite pores at suctions higher than the WEV. Thus, the water retention behaviour of the polymer masks the typical transition between the bentonite adsorption and capillary suction regime (as depicted by the WRC of GCL2), creating a more curvilinear shape at the WEV region.

#### 4.4. Geotextile pores

Due to the composite nature of GCL, it is postulated that macropores within the geotextile (GTX) dominate the water retention regime in the low suction range  $<1$  MPa. As the GCL undergoes wetting, the hydrating water will first fill up the bentonite pores, causing it to swell. Eventually, the suction of the GCL will correspond to the low suction region where capillary water fills the comparatively larger geotextile pores. This phenomenon is supported by the observations made in the data shown in Fig. 7. Note, however, the geotextile can also contribute to the water retention behaviour at the intermediate suctions when bentonite extrudes into the geotextile pores, as seen in Fig. 9.

Most GCLs experience increased volumetric water content in the very low suction range around 0.1–0.3 kPa, the exceptions being GCL3 and GCL4 (Figs. 6 and 7). This increase is due to the onset of water filling capillary pores, as characterised by a WEV for the GTX, leading to these GTX pores being saturated. This is consistent with the observations made by Bouazza et al. (2006a, 2006b), who reported water entry values for two geotextiles to be in the range of 0.2–0.3 kPa; whilst Iryo and Rowe (2003) indicated that most WEVs varied from 0 to 0.8 kPa.

For GCL3, no steep increase of VWC is observed in the low suction ranges, unlike the other GCLs. A probable explanation for this behaviour could be that when polymers react with water, they diffuse to the geotextile surface under low suctions (as observed in Fig. 8). When the suction measurements of GCL3 were taken at low suctions using IW-CFPT, it was observed that polymer had eluted to the surface of the geotextiles and created a film at the GCL surface. Because the filter papers were directly in contact with the polymer layer rather than the GCL, measurements were adversely impacted. As shown in Fig. 8a, this phenomenon was more evident in GCL3 (with high polymer content) probably because it contained highly water-soluble linear polymers rather than the crosslinked polymers found in GCL4 and GCL5. Thus, suction measurements conducted using the IW-CFPT could be considered as more reflective of the polymer water retention curve than the water retention behaviour of the GCL as a composite material shown in Fig. 7. As for GCL4, a slope was observed at higher suctions around the region of 30–50 kPa (Fig. 7), which is higher than typically expected for geotextile pores. However, GCL4 has a very high swelling capacity which might explain this phenomenon. In addition, during wetting at low suctions, hydrated polymer granules squeezed out of the geotextile fibres and accumulated within the geotextile pores. Thus, it is considered that the slope observed in the low suction range for GCL4 shown in Fig. 7 indicates that hydration and swelling of bentonites and polymers take place within the geotextile pores.

The proportion of geotextile pores is smaller than the bentonite pores in the GCL. Thus, the volumetric water content influx due to the capillary water of geotextile pores seen in 0.2 kPa suction range is not as drastic as the slope seen at 1 MPa due to the bentonite capillary water.

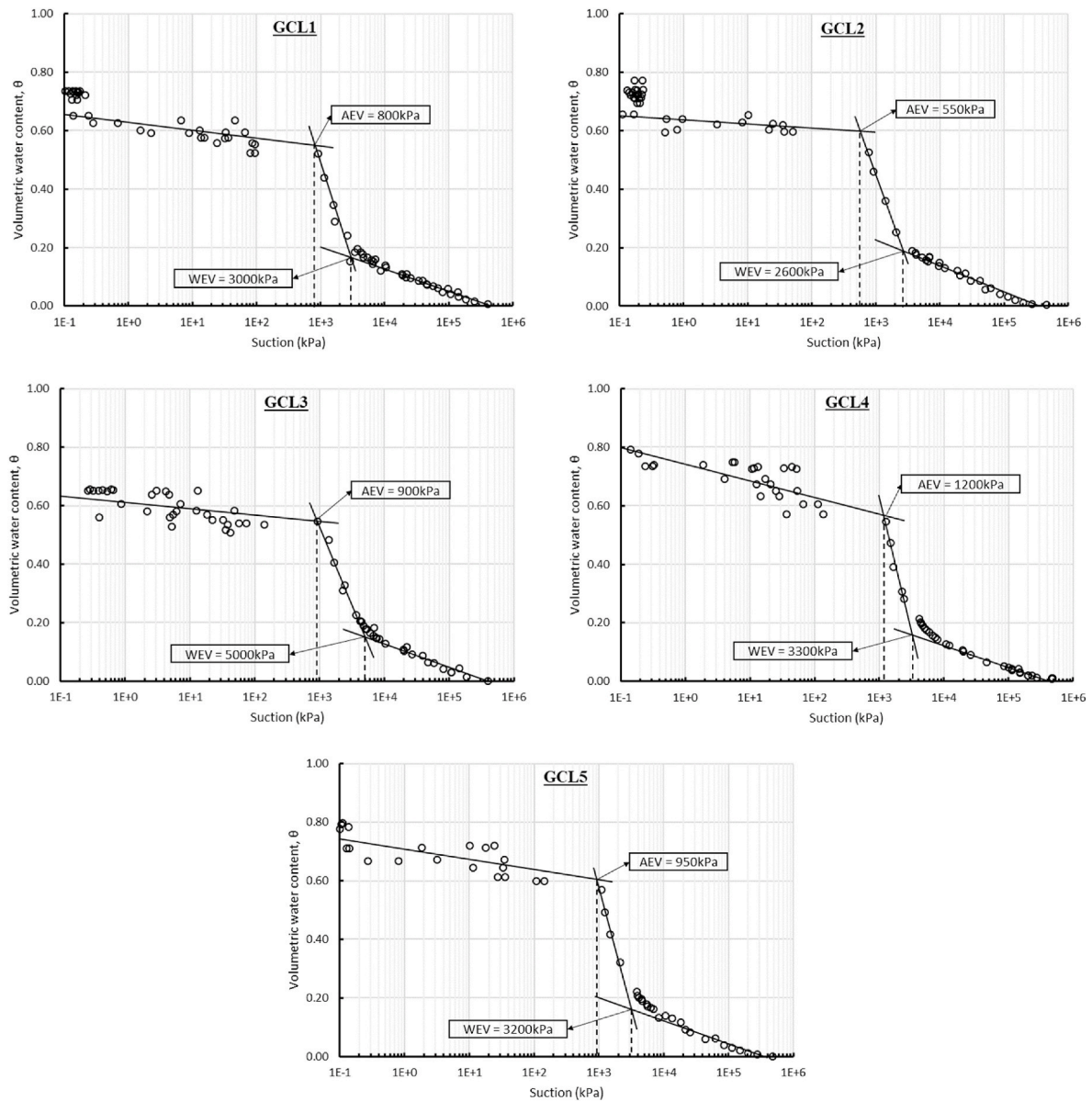


Fig. 6. Bentonite capillary zone for the various GCLs indicating air expulsion value (AEV) and water entry value (WEV). See Table 1 for polymer contents of the various GCLs.

Furthermore, the wetting path of the GCL WRC, as shown gravimetrically in Fig. 2a, depicts a proportionally larger increase for the slope in the geotextile regime compared to when shown volumetrically in Fig. 2b. This difference can be attributed to the large volume change that occurs in this region. As more water enters the GCL, the bentonite gradually swells and activates the geotextile fibres that confine it. Although they restrict the bentonite from freely swelling, the high swelling pressure at very low suctions causes the fibres to stretch out. Additionally, the bentonite swelling also results in the gradual intrusion of bentonite into the geotextile pores, where it absorbs more water. This is reflected in this region's relatively modest volumetric water content increase (Fig. 2b) despite the increase in gravimetric water content (Fig. 2a), accounting for almost 40% of the total gravimetric water content. Additionally, this also explains the slight incline in the GCL WRC across the whole low suction range (<146 kPa) instead of the presence of a flat plateau after the air expulsion value (AEV). Both phenomena (bentonite extrusion and geotextile fibre stretching/breakage) were observed by Gates et al. (2018) using micro XCT imaging. The high contrast cross-sectional XCT image of the GCL shown in

Fig. 9 shows the intrusion of hydrated bentonite into the nonwoven cover geotextile pores (indicated by the white box).

As discussed earlier, the low suction regime has been largely omitted in past studies on the water retention behaviour of GCLs, primarily due to reproducibility issues and the relatively small impact geotextiles have on the overall water retention behaviour. Nonetheless, a more in-depth understanding of the water retention regime in this suction range is crucial as it could shine some light on the phenomenon in which the final water content of the GCL on the wetting path is lower than its initial water content on the drying path. While typically attributed to air being trapped in voids during the wetting process, it is herein postulated that the lower final water content of the GCL on the wetting path could be a consequence of the GCL wetting path being terminated at a suction range before all the capillary pores in the geotextiles being filled. Thus, the difference in the water contents, in addition to possible entrapped air voids, is a remnant of an incomplete suction measurement range. This is supported by the measurements made in this study, as presented in Fig. 7, where a bimodal curve is observed when the WRC is shown up to 0.1 MPa.

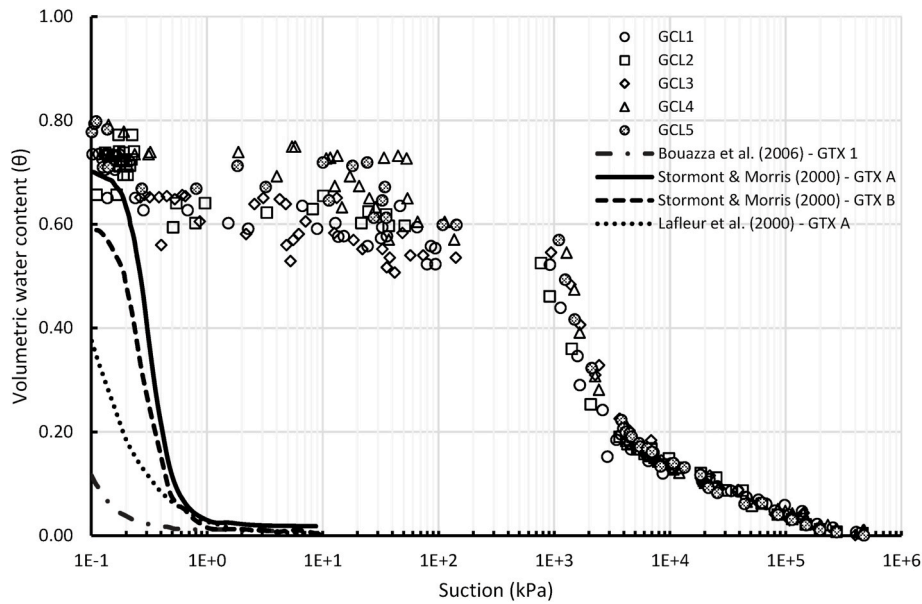


Fig. 7. Comparison between GCL WRCs and published geotextiles WRC data. See Table 1 for polymer contents of the various GCLs.

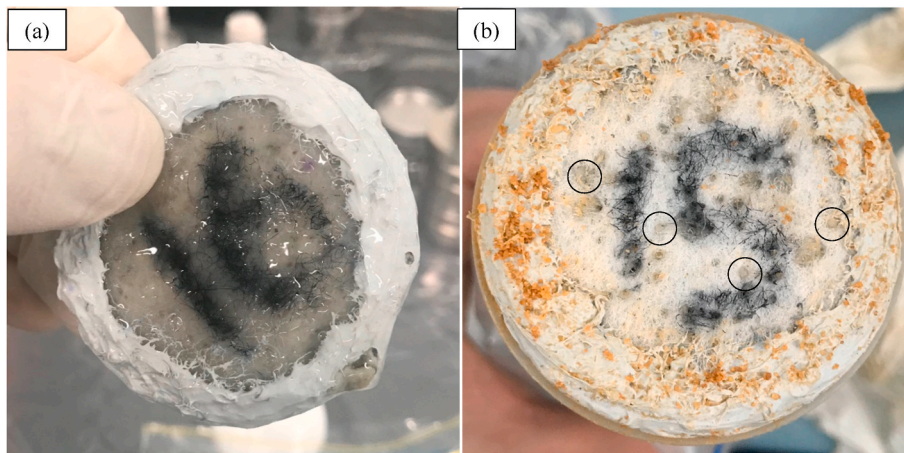


Fig. 8. Picture of (a) GCL3 with eluted polymer layer forming on the geotextile surface; (b) GCL4 with small, hydrated polymer granules indicated by the black circles forming in the geotextile pores.

#### 4.5. Water retention behaviour of polymer bentonite

There exists a lack of information regarding the water retention behaviour polymer enhanced bentonite. Water retention by various products would likely differ from one to the other due to the multitude of polymer types, polymer loading (Liu et al., 2012), and different manufacturing processes involved. Thus, to study the onset of hydraulic activation by the polymer in the polymer enhanced bentonite, an investigation into the water retention behaviour at the high suction range was made between GCL1, its unmodified base bentonite, and its raw polymer and a suite of dry blended polymer-bentonite mixtures. The results are presented in Fig. 10, where it can be observed that the polymer itself has a significantly higher water adsorption capacity compared to the bentonite component (Fig. 10a). Its water content at the lowest measured suction (7 MPa, equivalent to RH = 95%) is almost 17 times higher than the base bentonite at the same suction level. A comparison was also made between the dry blended polymer bentonite mixture and the base bentonite, as seen in Fig. 10b. The vapour sorption isotherms between the materials on the wetting path were largely identical to about 39 MPa suction (equivalent to RH of 75%). After

which, as the suction decreased, the polymer-modified bentonites (2.0%, 4.0% and 8.0% polymer bentonite mixtures) adsorbed appreciably more water. This point of divergence coincides with the region where the monolayer water adsorption around the exchangeable cation is completed, and beyond which it transitions to a two-layer hydrate state (Likos and Lu, 2002; Likos and Wayllace, 2010; Gates et al., 2017). The results shown in Fig. 10 are consistent with the findings reported in Akin and Likos (2016), which support the theory that the bentonite exchangeable cation hydration energies dominate the initial adsorption behaviour. The adsorption characteristics from active polymer sites only become apparent after the monolayer adsorption is completed in the bentonite. As the polymer starts to retain water, it forms a hydrogel structure around the bentonite particle or aggregate pores. It is hypothesised that such a situation applies to the dry-blended polymer bentonite mixtures, where the bentonite and polymer components are phase-separated and largely immiscible (Alexandre and Dubois, 2000). The water retention behaviour of the polymer and bentonite components thus function independently, where the moisture uptake of each component depends on its sorption strength. This also explains why the point of divergence of the polymer bentonite mixtures and the

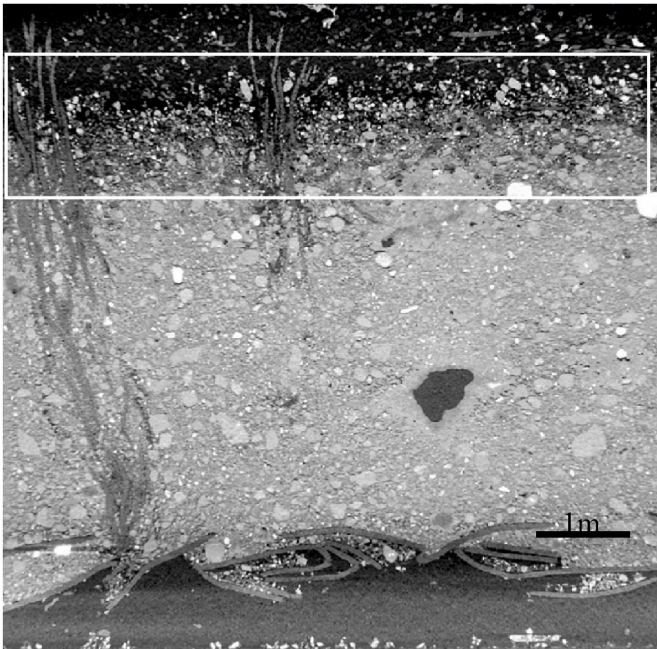


Fig. 9. High-resolution micro XCT image depicting the cross-section of a partially hydrated GCL (Gates et al., 2018).

unmodified base bentonite overlaps with the suction region, indicating the onset of significant moisture uptake for the pure polymer vapour sorption isotherm.

On the other hand, it was found that the moisture uptake of GCL1 at 7 MPa suction ( $RH = 95\%$ ) was lower than for the various polymer bentonite blends and even the base bentonite. On the wetting path, the GCL1 initially follows the same path as the other bentonite samples until a suction of 59 MPa ( $RH = 65\%$ ) where the path diverges, and GCL1 moisture adsorption becomes comparatively less. As GCL1 was manufactured using the same base bentonite and polymer, its mineralogical and chemical properties are similar to the various polymer bentonite blends. It can thus be posited that this phenomenon is due to the heating treatment of GCL1 during its manufacturing process, resulting in polymer adsorption where the polymer bentonite interaction changes at the vapour sorption range. It is possible that the polymers have intercalated and adsorbed to the bentonite interlayer surfaces due to the thermal treatment, therefore, ensuring that the water retention behaviour of the polymer and bentonite components function as a composite. As the vapour sorption range measured in this test is limited to  $RH = 95\%$ , it only captures up to two to three layers hydration state of the bentonite interlayer. It is believed that due to the manufacturing process, the polymer enhancement in the GCL1 will only become more dominant at lower suctions or possibly when there is capillarity. However, further studies need to be conducted to fully understand how the polymer bentonite's manufacturing process can impact its behaviour at the high suction range.

It is therefore hypothesised, as shown in the conceptual model illustrated in Fig. 3, that the onset of polymer water retention in polymer

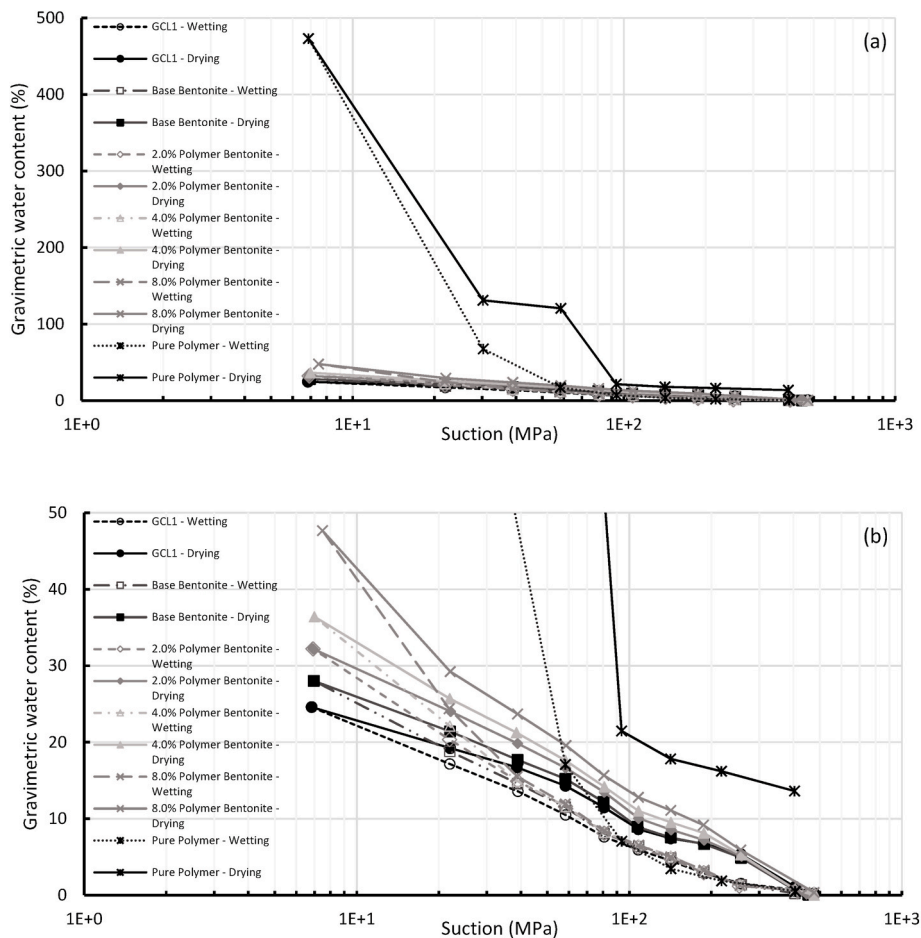


Fig. 10. Vapour sorption isotherm of (a) Pure polymer and various polymer bentonites, (b) GCL1 and the various polymer bentonite mixtures. See Table 1 for polymer contents of the various GCLs.

enhanced bentonite would occur as soon as possible after the monolayer water adsorption in the bentonite interlayer is completed, which corresponds to around 40 MPa ( $RH = 75\%$ ) for dry blended polymer bentonite mixtures, and at lower suctions for polymer bentonites like the GCL1. Nonetheless, it should be emphasised that this hydration mechanism for the polymer fraction in bentonite is unique to the specific polymer type, polymer dosage, and manufacturing process.

#### 4.6. Comparison with published data

Comparison with other water retention curves on the wetting path published in literature is presented in Fig. 11. The comparison was reported in terms of GWC as not all published data reported the WRCs volumetrically. The WRC wetting path of 2 powdered bentonite GCLs reported by Acikel et al. (2018b) were fitted using the Fredlund and Xing (1994) model (FX). The reported experimental data stopped at around 100 kPa, with the fitted curve extending to 10 kPa using measured saturated GWC. As discussed in the previous section, and shown in Fig. 11, omission of the low suction range data would bypass the suction behaviour of the geotextile. Hence, this would result in the fitted curve overestimating water content in the low suction range. Beddoe et al. (2011) reported the wetting path WRC of 4 GCLs that was measured using capacitance relative humidity sensors in the high suction range and high capacity tensiometers in the low suction range. The data were curve fitted using the FX model as well. The lower bound of the reported suction measurements and fitted curve was set at 1 kPa. There were no measurements made in the intermediate suction range where the capillary zone of the bentonite is dominant. Thus, the shape of the fitted curve is less defined in an area where there are significant water volume changes. Consequently, the output fitted parameters  $a$  and  $\psi_r$  would not provide values with relevant physical explanations. Comparing these literature data with the experimental data obtained in this study highlights the importance of having measurements for GCL over a wide range of suction to fully capture its water retention behaviour, understanding that it is affected by multiple different suction regimes. It also highlights the limitations of commonly used unimodal fitting curves in predicting the water retention behaviour of GCL, especially when having to account for its bimodal nature. Thus, this study provides the experimental data and framework to assess and validate a proposed fitting model for GCL water retention behaviour in future work.

## 5. Conclusions

This study was undertaken to provide greater insight into the wetting path water retention behaviour of GCLs through the framework of their pore structures and resulting suction regimes. The theoretical explanations were provided alongside the experimental WRC data measured for the GCLs used in this study. Due to the composite nature of GCLs, a combination of test methods like the vapour sorption method, vapour equilibrium technique, chilled mirror hygrometer method, and the initial wet contact filter paper test was used to chart out water retention behaviour fully. The salient conclusions that can be drawn for this work include:

1. When measured across an extended suction range which includes suction  $< 10$  kPa, it was observed that GCLs exhibit a bimodal curve (trimodal if considering the bentonite micropores and macropores as separate pore structures) on the wetting path consistent with its composite nature where the geotextiles and bentonite component have widely different pore sizes. The water retention behaviour of GCLs can be explained through their pore structures, from smallest to largest: bentonite micropores, bentonite macropores and geotextile pores.
2. The results indicate that the water retention properties of the GCLs and their bentonite component were very similar. The high suction regime, where the bentonite micropores are dominant, comprises the tightly adsorbed and adsorbed film regime with adsorption water, which is largely responsible for any water change. GCL4 was an exception, likely due to its high polymer loading and high swelling behaviour, which indicates the onset of geotextile confinement at higher suctions. Overall, this study showed that the behaviour of GCLs in the high suction range was almost entirely governed by the bentonite fraction, consistent with other literature findings.
3. Bentonite macropores dictate the water retention behaviour in the intermediate suction range (between 1 and 20,000 kPa depending on the water entry values). As the water in the system reaches its adsorption capacity, the main water intake is mainly comprised of capillary water in the inter-aggregate pores. The behaviour of the GCL diverges from pure bentonite due to the confinement provided by the geotextile fibres. Its air expulsion value demarcates this regime's boundaries, and the water entry value was shown to occur at suctions lower than the pore water's cavitation suction. It was found

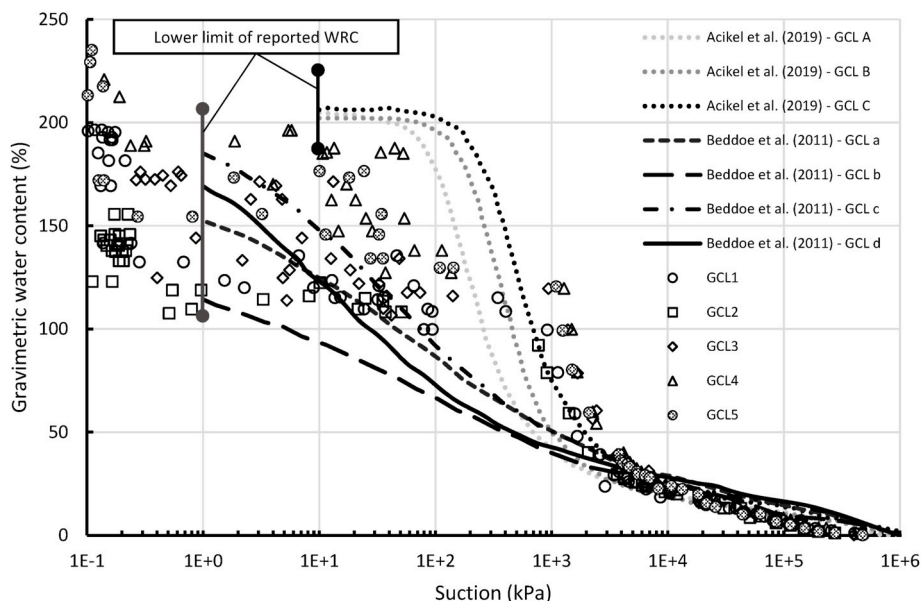


Fig. 11. Comparison with published literature data.

that GCLs with higher polymer loading tend to have higher WEV and AEV. It indicates that the increased water uptake by the polymer modified bentonite has led to the onset of water entry into the bentonite capillary pores and expulsion of voids from said pores at higher suctions.

4. The WRC of the GCL indicates that the geotextile pores influence the low suction range behaviour. The WEV of the slope in the low suction range is around 0.2 kPa, consistent with literature data. The capillary water retained in the geotextile pores can account partially for the gap between the final water content of the GCL on the wetting path and the initial water content on the drying path. Other contributory factors for water uptake in the low suction range include bentonite swelling and extrusion and polymer water adsorption. The relatively modest volumetric water content increase in this region despite the increase in gravimetric water content in the same region, accounting for almost 40% of the total gravimetric water content, still indicates that the GCL undergoes large volume changes. It also explains the slight incline in the GCL V-WRC across the low suction range beyond the AEV.
5. The polymer loading can impact the dominant hydraulic mechanism of the polymer bentonite. If polymer additives are present, their effect becomes more apparent after the completion of monolayer cation hydration. Due to its higher water sorption capacity, the most evident impact of polymer modifications on GCL hydration is the

increased water uptake. For GCL1, it was found that it was still dictated by osmotic swelling and its polymer bentonite interactions serve to promote this mechanism. Furthermore, it was found that onset of polymer water retention in polymer enhanced bentonite would occur at the earliest after the monolayer water adsorption in the bentonite interlayer is completed, which corresponds to around 40 MPa (RH = 75%) for dry blended polymer bentonite mixtures, and at lower suctions for polymer bentonites like the GCL1. It should be emphasised that the hydration mechanism for the polymer fraction in bentonite is unique to the specific polymer type, polymer dosage, and manufacturing process.

This paper shows that the water retention behaviour of GCL can be wholly explained by the influence of its pore structures within various suction regimes. Current models are inadequate at capturing the full water retention behaviour of the GCL considering its composite nature. A bimodal general equation would be a more suitable solution for describing the water retention regimes of a GCL.

#### Acknowledgement

This research project was supported by the Australian Research Council's Discovery Projects funding scheme (project number DP190103682). This support is gratefully acknowledged.

#### Acronyms

<b>AEV</b>	Air expulsion value
<b>ASTM</b>	American standard testing methods
<b>BPA</b>	Bentonite polymer alloy
<b>BPB</b>	Bentonite polymer nanocomposite
<b>CEC</b>	Cation exchange capacity
<b>DPH</b>	Dense pre-hydrated
<b>DVS</b>	Dynamic vapour sorption
<b>FX</b>	<a href="#">Fredlund and Xing (1994)</a> .
<b>GC</b>	Glycerol carbonate
<b>GCL</b>	Geosynthetic clay liner
<b>GMB</b>	Geomembrane
<b>GTX</b>	Geotextile
<b>GWC</b>	Gravimetric water content
<b>GWRC</b>	Gravimetric water retention curve
<b>IWCFPT</b>	Initial wet contact filter paper test
<b>MSB</b>	Multi-swellable bentonite
<b>Na-CMC</b>	Sodium carboxymethyl cellulose
<b>PAA</b>	Anionic acrylic polymer
<b>PAC</b>	Polyanionic cellulose
<b>PAM</b>	Polyacrylamide
<b>PC</b>	Propylene carbonate
<b>RH</b>	Relative humidity
<b>RSS</b>	Residual sum of squares
<b>SEM</b>	Scanning electron microscopy
<b>SI</b>	Swell index
<b>VET</b>	Vapour equilibrium technique
<b>VG</b>	<a href="#">Van Genuchten (1980)</a>
<b>VSA</b>	Vapour sorption analyser
<b>VWC</b>	Volumetric water content
<b>VWRC</b>	Volumetric water retention curve
<b>WEV</b>	Water entry value
<b>WRC</b>	Water retention curve
<b>XCT</b>	X-ray computed tomography
<b>XRD</b>	X-ray diffraction

#### Notations

$\sigma_c$	Cavitation deviation
------------	----------------------

a	Air expulsion value
m	Curve fitting parameter related to overall WRC geometry
n	Curve fitting parameter related to pore size distribution
R2	Coefficient of correlation
$\alpha$	Inverse of AEV
$\theta$	Volumetric water content
$\theta_a$	Adsorption water content
$\theta_{\max}$	Total adsorption water capacity
$\theta_c$	Capillary water content
$\theta_r$	Residual water content
$\theta_s$	Saturated water content
$\psi$	Suction
$\psi_c$	Mean cavitation suction
$\psi_{\max}$	Maximum suction value
$\psi_r$	Suction value corresponding to residual water content

## References

- Abuel-Naga, H.M., Bouazza, A., 2010. A novel laboratory technique to determine the water retention curve of geosynthetic clay liners. *Geosynth. Int.* 17 (5), 313–322.
- Abuel-Naga, H.M., Bouazza, A., 2013. Thermomechanical behavior of saturated geosynthetic clay liners. *J. Geotech. Geoenviron. Eng.* 139 (4), 539–547.
- Acikel, A.S., 2016. *Unsaturated Behaviour of Geosynthetic Clay Liners*. PhD Thesis. Department of Civil Engineering, Monash University, Melbourne, Australia. <https://doi.org/10.4225/03/585085cce89ba>.
- Acikel, A.S., Bouazza, A., Gates, W.P., Singh, R.M., Rowe, R.K., 2020. A novel transient gravimetric monitoring technique implemented to GCL osmotic suction control. *Geotext. Geomembranes* 48 (6), 755–767.
- Acikel, A.S., Bouazza, A., Singh, R.M., Gates, W.P., Rowe, R.K., 2022. Challenges of the filter paper suction measurements in geosynthetic clay liners: effects of method, time, capillarity, and hysteresis. *Geotech. Test J.* 45 (21), GTJ20200168.
- Acikel, A.S., Gates, W.P., Singh, R.M., Bouazza, A., Rowe, R.K., 2018a. Insufficient initial hydration of GCLs from some subgrades: factors and causes. *Geotext. Geomembranes* 46 (6), 770–781.
- Acikel, A.S., Gates, W.P., Singh, R.M., Bouazza, A., Fredlund, D.G., Rowe, R.K., 2018b. Time-dependent unsaturated behaviour of geosynthetic clay liners. *Can. Geotech. J.* 55 (12), 1824–1836.
- Acikel, A.S., Singh, R.M., Bouazza, A., Gates, W.P., Rowe, R.K., 2011. Water retention behaviour of unsaturated geosynthetic clay liners. In: *Proceedings of 13th International Conference of the International Association for Computer Methods and Advances in Geomechanics*, pp. 626–630.
- Acikel, A.S., Singh, R.M., Bouazza, A., Gates, W.P., Rowe, R.K., 2015. Applicability and accuracy of the initially dry and initially wet contact filter paper tests for matrix suction measurement of geosynthetic clay liners. *Geotechnique* 65 (9), 780–787.
- Akin, I.D., Likos, W.J., 2016. Water vapor sorption of polymer-modified bentonites. In *Geo-Chicago* 508–517.
- Alexandre, M., Dubois, P., 2000. Polymer-layered silicate nanocomposites: preparation, properties and uses of a new class of materials. *Mater. Sci. Eng. R Rep.* 28 (1–2), 1–63.
- Alonso, E.E., Vaunat, J., Gens, A., 1999. Modelling the mechanical behaviour of expansive clays. *Eng. Geol.* 54 (1–2), 173–183.
- Anderson, R., Rayhani, M.T., Rowe, R.K., 2012. Laboratory investigation of GCL hydration from clayey sand subsoil. *Geotext. Geomembranes* 31, 31–38.
- ASTM: D5298, 2016. Standard Test Method for Measurement of Soil Potential (Suction) Using Filter Paper. ASTM International, West Conshohocken, PA.
- ASTM: D5890, 2008. Standard Test Method for Swell Index of Clay Mineral Component of Geosynthetic Clay Liners. ASTM International, West Conshohocken, PA.
- ASTM: D5891, 2008. Standard Test Method for Fluid Loss of Clay Component of Geosynthetic Clay Liners. ASTM International, West Conshohocken, PA.
- ASTM: D5993, 2008. Standard Test Method for Measuring Mass Per Unit of Geosynthetic Clay Liners. ASTM International, West Conshohocken, PA.
- ASTM: D7503, 2018. Standard Test Method for Measuring the Exchange Complex and Cation Exchange Capacity of Inorganic Fine-Grained Soils. ASTM International, West Conshohocken, PA.
- ASTM: E104, 2007. Standard Practice for Maintaining Constant Relative Humidity by Means of Aqueous Solutions. ASTM International, West Conshohocken, PA.
- Bannour, H., Stoltz, G., Delage, P., Touze-Foltz, N., 2014. Effect of stress on water retention of needle-punched geosynthetic clay liners. *Geotext. Geomembranes* 42, 629–640.
- Barclay, A., Rayhani, M.T., 2013. Effect of temperature on hydration of geosynthetic clay liners in landfills. *Waste Manag. Res.* 31 (3), 265–272.
- Barroso, M., Touze-Foltz, N., Saidi, F.K., 2006. Validation of the use of filter paper suction measurements for the determination of GCL water retention curves. In: *Proceedings of the 8th International Conference on Geosynthetics*, Yokohama, pp. 171–174.
- Battaglia, S., Leoni, L., Sartori, F., 2006. A method for determining the CEC and chemical composition of clays via XRF. *Clay Miner.* 41 (3), 717–725.
- Beddoe, R.A., Rowe, R.K., Take, W.A., 2010. Development of suction measurement techniques to quantify the water retention behaviour of GCLs. *Geosynth. Int.* 17 (5), 301–312.
- Beddoe, R.A., Take, W.A., Rowe, R.K., 2011. Water-retention behavior of geosynthetic clay liners. *J. Geotech. Geoenviron. Eng.* 137 (11), 1028–1038.
- Bohnhoff, G.L., Shackelford, C.D., 2014. Hydraulic conductivity of chemically modified bentonites for containment barriers. In: *7th International Congress on Environmental Geotechnics: Iceg2014*, pp. 440–447 (Engineers Australia).
- Bordallo, H.N., Aldridge, L.P., Churchman, G.J., Gates, W.P., Telling, M.T., Kiefer, K., et al., 2008. Quasi-elastic neutron scattering studies on clay interlayer-space highlighting the effect of the cation in confined water dynamics. *J. Phys. Chem. C* 112 (36), 13982–13991.
- Bouazza, A., 2002. Geosynthetic clay liners. *Geotext. Geomembranes* 20 (1), 3–17.
- Bouazza, A., 2021. Interaction between PFASs and geosynthetic liners: current status and the way forward. *Geosynth. Int.* 28 (2), 214–223.
- Bouazza, A., Bowders Jr., J.J., 2009. *Geosynthetic Clay Liners for Waste Containment Facilities*. CRC Press, London.
- Bouazza, A., Gates, W.P., 2014. Overview of performance compatibility issues of GCLs with respect to leachates of extreme chemistry. *Geosynth. Int.* 21 (2), 151–167.
- Bouazza, A., Rouf, M.A., 2021. Hysteresis of the water retention curves of geosynthetic clay liners in the high suction range. *Geotext. Geomembranes* 49 (4), 1079–1084.
- Bouazza, A., Freund, M., Nahlawi, H., 2006a. Water retention of nonwoven polyester geotextiles. *Polym. Test.* 25 (8), 1038–1043.
- Bouazza, A., Zornberg, J.G., McCartney, J.S., Nahlawi, H., 2006b. Significance of unsaturated behaviour of geotextiles in earthen structures. *Aust. Geomech J.* 41 (3), 133–142.
- Bouazza, A., Ali, M.A., Gates, W.P., Rowe, R.K., 2017a. New insight on geosynthetic clay liner hydration: the key role of subsoils mineralogy. *Geosynth. Int.* 24 (2), 139–150.
- Bouazza, A., Ali, M.A., Rowe, R.K., Gates, W.P., El-Zein, A., 2017b. Heat mitigation in geosynthetic composite liners exposed to elevated temperatures. *Geotext. Geomembranes* 45 (5), 406–417.
- Bradshaw, S.L., Benson, C.H., Scalia IV, J., 2013. Hydration and cation exchange during subgrade hydration and effect on hydraulic conductivity of geosynthetic clay liners. *J. Geotech. Geoenviron. Eng.* 139 (4), 526–538.
- Burger, C.A., Shackelford, C.D., 2001. Evaluating dual porosity of pelletised diatomaceous earth using bimodal soil-water characteristic curve functions. *Can. Geotech. J.* 38 (1), 53–66.
- Carnero-Guzman, G.G., Gates, W.P., Bouazza, A., Aldridge, L.P., Bordallo, H.N., 2019. Using neutron spectroscopy to measure soil-water retention at high suction ranges. *Can. Geotech. J.* 56 (12), 1999–2003.
- Carnero-Guzman, G.G., Bouazza, A., Gates, W.P., Rowe, R.K., McWatters, R., 2021. Hydration/dehydration behaviour of geosynthetic clay liners in the Antarctic environment. *Geotext. Geomembranes* 49 (1), 196–209.
- Chen, J., Salihoglu, H., Benson, C.H., Likos, W.J., Edil, T.B., 2019. Hydraulic conductivity of bentonite-polymer composite geosynthetic clay liners permeated with coal combustion product leachates. *J. Geotech. Geoenviron. Eng.* 145 (9), 04019038.
- Chevrier, B., Cazaux, D., Didier, G., Gamet, M., Guyonnet, D., 2012. Influence of subgrade, temperature and confining pressure on GCL hydration. *Geotext. Geomembranes* 33, 1–6.
- Cui, Y.J., 2017. On the hydro-mechanical behaviour of MX80 bentonite-based materials. *Journal of Rock Mechanics and Geotechnical Engineering* 9 (3), 565–574.
- De Camillis, M., Di Emidio, G., Bezuijen, A., Verastegui-Flores, R.D., 2016. Hydraulic conductivity and swelling ability of a polymer modified bentonite subjected to wet-dry cycles in seawater. *Geotext. Geomembranes* 44 (5), 739–747.
- Delage, P., 2007. Microstructure features in the behaviour of engineered barriers for nuclear waste disposal. In: *Experimental Unsaturated Soil Mechanics*. Springer, Berlin, Heidelberg, pp. 11–32.
- Di Emidio, G., Mazzieri, F., Verastegui-Flores, R.D., Van Impe, W., Bezuijen, A., 2015. Polymer-treated bentonite clay for chemical-resistant geosynthetic clay liners. *Geosynth. Int.* 22 (1), 125–137.

- Di Emidio, G., Van Impe, W.F., Flores, R.V., 2011. Advances in geosynthetic clay liners: polymer enhanced clays. In: *Geo-Frontiers 2011: Advances in Geotechnical Engineering*, pp. 1931–1940.
- Ernstsen, V., Gates, W.P., Stucki, J.W., 1998. Microbial reduction of structural iron in clays—a renewable source of reduction capacity. *J. Environ. Qual.* 27 (4), 761–766.
- Fehervari, A., Gates, W.P., Patti, A.F., Turney, T.W., Bouazza, A., Rowe, R.K., 2016. Potential hydraulic barrier performance of cyclic organic carbonate modified bentonite complexes against hyper-salinity. *Geotext. Geomembranes* 44 (5), 748–760.
- Fredlund, D.G., Xing, A., 1994. Equations for the soil-water characteristic curve. *Can. Geotech. J.* 31 (4), 521–532.
- Fredlund, D.G., Rahardjo, H., Fredlund, M.D., 2012. *Unsaturated Soil Mechanics in Engineering Practice*. John Wiley & Sons, Inc. <https://doi.org/10.1002/9781118280492>.
- Frydman, S., Baker, R., 2009. Theoretical soil-water characteristic curves based on adsorption, cavitation, and a double porosity model. *Int. J. GeoMech.* 9 (6), 250–257.
- Gates, W.P., Bordallo, H.N., Aldridge, L.P., Seydel, T., Jacobsen, H., Marry, V., Churchman, G.J., 2012. Neutron time-of-flight quantification of water desorption isotherms of montmorillonite. *J. Phys. Chem. C* 116 (9), 5558–5570.
- Gates, W.P., Bordallo, H.N., Bouazza, A., Carnero-Guzman, G.G., Aldridge, L.P., Klapproth, A., Iles, G.N., Booth, N., Mole, R.A., Seydel, T., Yu, D., de Souza, N.R., 2021. Neutron scattering quantification of unfrozen pore water in frozen mud. *Microporous Mesoporous Mater.*, 111267.
- Gates, W.P., Dumadah, G., Bouazza, A., 2018. Micro X-ray visualisation of the interaction of geosynthetic clay liner components after partial hydration. *Geotext. Geomembranes* 46 (6), 739–747.
- Gates, W.P., Hornsey, W.P., Buckley, J.L., 2009. Geosynthetic clay liners - is the key component being overlooked. In: *Proceeding of GIGSA GeoAfrica 2009 Conference*, Cape Town.
- Gates, W.P., Aldridge, L.P., Carnero-Guzman, G.G., Mole, R.A., Yu, D., Iles, G.N., Klapproth, A., Bordallo, H.N., 2017. Water desorption and absorption isotherms of sodium montmorillonite: a QENS study. *Appl. Clay Sci.* 147, 97–104.
- Gates, W.P., MacLeod, A., Fehervari, A., Bouazza, A., Gibbs, D., Hackney, R., Callahan, D. L., Watts, M., 2020. Interactions of per-and polyfluoralkyl substances (PFAS) with landfill liners. *Advances in Environmental and Engineering Research* 1 (4).
- Gens, A., Alonso, E.E., 1992. A framework for the behaviour of unsaturated expansive clays. *Can. Geotech. J.* 29 (6), 1013–1032.
- Ghavam-Nasiri, A., El-Zein, A., Airey, D., Rowe, R.K., 2019. Water retention of geosynthetic clay liners: dependence on void ratio and temperature. *Geotext. Geomembranes* 47 (2), 255–268.
- Ghavam-Nasiri, A., El-Zein, A., Airey, D., Rowe, R.K., Bouazza, A., 2020. Thermal desiccation of geosynthetic clay liners under brine pond conditions. *Geosynth. Int.* 27 (6), 593–605.
- Herbert, E., Balibar, S., Caupin, F., 2006. Cavitation pressure in water. *Phys. Rev.* 74 (4), 041603.
- Hornsey, W.P., Scheirs, J., Gates, W.P., Bouazza, A., 2010. The impact of mining solutions/liquors on geosynthetics. *Geotext. Geomembranes* 28 (2), 191–198.
- Iryo, T., Rowe, R.K., 2003. On the hydraulic behavior of unsaturated nonwoven geotextiles. *Geotext. Geomembranes* 21 (6), 381–404.
- Israelachvili, J.N., 2011. *Intermolecular and Surface Forces*, third ed. Elsevier, Amsterdam, Netherlands.
- Jensen, D.K., Tuller, M., de Jonge, L.W., Arthur, E., Moldrup, P., 2015. A new two-stage approach to predicting the soil water characteristic from saturation to oven-dryness. *J. Hydrol.* 521, 498–507.
- Katsumi, T., Ishimori, H., Onikata, M., Fukagawa, R., 2008. Long-term barrier performance of modified bentonite materials against sodium and calcium permeant solutions. *Geotext. Geomembranes* 26 (1), 14–30.
- Khorshidi, M., Lu, N., Akin, I.D., Likos, W.J., 2017. Intrinsic relationship between specific surface area and soil water retention. *J. Geotech. Geoenviron. Eng.* 143 (1), 04016078.
- Kuligiewicz, A., Derkowski, A., 2017. Tightly bound water in smectites. *Am. Mineral.* 102 (5), 1073–1090.
- Laird, D.A., 1996. Model for crystalline swelling of 2: 1 phyllosilicates. *Clay Clay Miner.* 44 (4), 553–559.
- Lau, Z.C., Bouazza, A., Gates, W.P., 2022. Water exchange across a subgrade-GCL interface as impacted by polymers and environmental conditions. *Geotext. Geomembranes* 50 (1), 40–54.
- Leong, E.C., He, L., Rahardjo, H., 2002. Factors affecting the filter paper method for total and matric suction measurements. *Geotech. Test J.* 25 (3), 322–333.
- Li, Q., Chen, J., Benson, C.H., Peng, D., 2021. Hydraulic conductivity of bentonite-polymer composite geosynthetic clay liners permeated with bauxite liquor. *Geotext. Geomembranes* 49 (2), 420–429.
- Likos, W.J., Lu, N., 2002. Water vapor sorption behaviour of smectite-kaolinite mixtures. *Clay Clay Miner.* 50 (5), 553–561.
- Likos, W.J., Lu, N., 2006. Pore-scale analysis of bulk volume change from crystalline interlayer swelling in Na<sup>+</sup> and Ca<sup>2+</sup>-smectite. *Clay Clay Miner.* 54 (4), 515–528.
- Likos, W.J., Wayllace, A., 2010. Porosity evolution of free and confined bentonites during interlayer hydration. *Clay Clay Miner.* 58 (3), 399–414.
- Likos, W., Bowders, J., Gates, W., 2010. Mineralogy and engineering properties of bentonite. In: *Geosynthetic Clay Liners for Waste Containment Facilities*. CRC Press, pp. 31–53.
- Liu, J., Song, S., Cao, X., Meng, Q., Pu, H., Wang, Y., Liu, J., 2020. Determination of full-scale pore size distribution of Gaomiaozhi bentonite and its permeability prediction. *Journal of Rock Mechanics and Geotechnical Engineering* 12 (2), 403–413.
- Liu, Y., Gates, W.P., Bouazza, A., 2012. Improvement on the performance of geosynthetic clay liners using polymer modified bentonite. *Geotech. Eng.* 43 (3), 43–45.
- Liu, Y., Bouazza, A., Gates, W.P., Rowe, R.K., 2015. Hydraulic performance of geosynthetic clay liners to sulfuric acid solutions. *Geotext. Geomembranes* 43 (1), 14–23.
- Lu, N., 2016. Generalised soil water retention equation for adsorption and capillarity. *J. Geotech. Geoenviron. Eng.* 142 (10), 04016051.
- Lu, N., Khorshidi, M., 2015. Mechanisms for soil-water retention and hysteresis at high suction range. *J. Geotech. Geoenviron. Eng.* 141 (8), 04015032.
- Lu, Y., Abuel-Naga, H., Bouazza, A., 2017. Water retention curve of GCLs using a modified sample holder in a chilled-mirror dew-point device. *Geotext. Geomembranes* 45 (1), 23–28.
- Lu, Y., Abuel-Naga, H., Leong, E.C., Bouazza, A., Lock, P., 2018. Effect of water salinity on the water retention curve of geosynthetic clay liners. *Geotext. Geomembranes* 46 (6), 707–714.
- McWatters, R.S., Rowe, R.K., Wilkins, D., Spedding, T., Jones, D., Wise, L., Mets, J., Terry, D., Hince, G., Gates, W.P., Di Battista, V., Shoaib, M., Bouazza, A., Snape, I., 2016. Geosynthetics in Antarctica: performance of a composite barrier system to contain hydrocarbon-contaminated soil after three years in the field. *Geotext. Geomembranes* 44 (5), 673–685.
- Mazzieri, F., Emidio, G.D., 2015. Hydraulic conductivity of a dense prehydrated geosynthetic clay liner. *Geosynth. Int.* 22 (1), 138–148.
- Mazzieri, F., Di Emidio, G., Pasqualini, E., 2017. Effect of wet-and-dry ageing in seawater on the swelling properties and hydraulic conductivity of two amended bentonites. *Appl. Clay Sci.* 142, 40–51.
- McQueen, I.S., Miller, R.F., 1974. Approximating soil moisture characteristics from limited data: empirical evidence and tentative model. *Water Resour. Res.* 10 (3), 521–527.
- Mooney, R.W., Keenan, A.G., Wood, L.A., 1952. Adsorption of water vapor by montmorillonite. II. Effect of exchangeable ions and lattice swelling as measured by X-ray diffraction. *J. Am. Chem. Soc.* 74 (6), 1371–1374.
- Navarro, V., Asensio, L., De la Morena, G., Pintado, X., Yustres, A., 2015. Differentiated intra- and inter-aggregate water content models of mx-80 bentonite. *Appl. Clay Sci.* 118, 325–336.
- Norrish, K., 1954. The swelling of montmorillonite. *Discuss. Faraday Soc.* 18, 120–134.
- Norrish, K., Hutton, J.T., 1969. An accurate X-ray spectrographic method for the analysis of a wide range of geological samples. *Geochem. Cosmochim. Acta* 33 (4), 431–453.
- Or, D., Tuller, M., 2002. Cavitation during desaturation of porous media under tension. *Water Resour. Res.* 38 (5), 19–19–14.
- Ozhan, H.O., 2018. Hydraulic capability of polymer-treated GCLs in saline solutions at elevated temperatures. *Appl. Clay Sci.* 161, 364–373.
- Pasha, A.Y., Khoshghalb, A., Khalili, N., 2017. Hysteretic model for the evolution of water retention curve with void ratio. *J. Eng. Mech.* 143 (7), 04017030.
- Rayhani, M.H.T., Rowe, R.K., Brachman, R.W.L., Siemens, G., Take, A., 2008. Closed-system investigation of GCL hydration from subsoil. In: *61st Canadian Geotechnical Conference*, pp. 324–328.
- Rayhani, M.T., Rowe, R.K., Brachman, R.W.L., Take, W.A., Siemens, G., 2011. Factors affecting GCL hydration under isothermal conditions. *Geotext. Geomembranes* 29 (6), 525–533.
- Revil, A., Lu, N., 2013. Unified water isotherms for clayey porous materials. *Water Resour. Res.* 49 (9), 5685–5699.
- Romero, E., Della Vecchia, G., Jommi, C., 2011. An insight into the water retention properties of compacted clayey soils. *Geotechnique* 61 (4), 313–328.
- Rouf, M.A., Bouazza, A., Singh, R.M., Gates, W.P., Rowe, R.K., 2016. Water vapour adsorption and desorption in GCLs. *Geosynth. Int.* 23 (2), 86–99.
- Rouf, M.A., Singh, R.M., Bouazza, A., Gates, W.P., Rowe, R.K., 2014. Evaluation of a geosynthetic clay liner water retention curve using vapour equilibrium technique. In: *Proceedings of the 6th International Conference on Unsaturated Soils, UNSAT*, pp. 1003–1009.
- Rowe, R.K., 2013. Recent advances in understanding and improving the performance of lining and capping systems for landfill and mining applications. In: *Coupled Phenomena in Environmental Geotechnics*, CRC Press Taylor & Francis Group, pp. 3–20.
- Rowe, R.K., 2014. Performance of GCLs in liners for landfill and mining applications. *Environmental Geotechnics* 1 (1), 3–21.
- Rowe, R.K., AbdelRazek, A.Y., 2021. Performance of multicomponent GCLs in high salinity impoundment applications. *Geotext. Geomembranes* 49 (2), 358–368.
- Rowe, R.K., Rayhani, M.T., Take, W.A., Siemens, G., Brachman, R.W.L., 2011. GCL hydration under simulated daily thermal cycles. *Geosynth. Int.* 18 (4), 196–205.
- Saiyouri, N., Tessier, D., Hicher, P.Y., 2004. Experimental study of swelling in unsaturated compacted clays. *Clay Miner.* 39 (4), 469–479.
- Salihoglu, H., Chen, J.N., Likos, W.J., Benson, C.H., 2016. Hydraulic conductivity of bentonite-polymer geosynthetic clay liners in coal combustion product leachates. In: *Geo-Chicago* 438–447.
- Sanchez, M., Gens, A., Guimaraes, L., Olivella, S., 2006. Response of an unsaturated expansive clay under high temperature changes. In: *Unsaturated Soils 2006*, pp. 2488–2499.
- Sánchez, M., Gens, A., Villar, M.V., Olivella, S., 2016. Fully coupled thermo-hydro-mechanical double-porosity formulation for unsaturated soils. *Int. J. GeoMech.* 16 (6), D4016015.
- Sarabian, T., Rayhani, M.T., 2013. Hydration of geosynthetic clay liners from clay subsoil under simulated field conditions. *Waste Manag.* 33 (1), 67–73.
- Satyanaga, A., Rahardjo, H., Leong, E.C., Wang, J.Y., 2013. Water characteristic curve of soil with bimodal grain-size distribution. *Comput. Geotech.* 48, 51–61.

- Scalia, J., Benson, C.H., 2014. Barrier performance of bentonite-polyacrylate nanocomposite to artificial ocean water. In: *Geo-Congress 2014: Geo-Characterization and Modeling for Sustainability*, pp. 1826–1835.
- Scalia, J., Benson, C.H., Bohnhoff, G.L., Edil, T.B., Shackelford, C.D., 2014. Long-term hydraulic conductivity of a bentonite-polymer composite permeated with aggressive inorganic solutions. *J. Geotech. Geoenviron. Eng.* 140 (3), 04013025.
- Scalia, J., Bohnhoff, G.L., Shackelford, C.D., Benson, C.H., Sample-Lord, K.M., Malusis, M.A., Likos, W.J., 2018. Enhanced bentonites for containment of inorganic waste leachates by GCLs. *Geosynth. Int.* 25 (4), 392–411.
- Seiphoori, A., Ferrari, A., Laloui, L., 2014. Water retention behaviour and microstructural evolution of MX-80 bentonite during wetting and drying cycles. *Geotechnique* 64 (9), 721–734.
- Seiphoori, A., Laloui, L., Ferrari, A., Hassan, M., Khushefati, W.H., 2016. Water retention and swelling behaviour of granular bentonites for application in Geosynthetic Clay Liner (GCL) systems. *Soils Found.* 56 (3), 449–459.
- Southen, J.M., Rowe, R.K., 2007. Evaluation of the water retention curve for geosynthetic clay liners. *Geotext. Geomembranes* 25, 2–9.
- Sumner, M.E., Miller, W.P., 1996. Cation exchange capacity and exchange coefficients. *Methods of Soil Analysis: Part 3 Chemical Methods* 5, 1201–1229.
- Tian, K., Benson, C.H., Likos, W.J., 2016. Hydraulic conductivity of geosynthetic clay liners to low-level radioactive waste leachate. *J. Geotech. Geoenviron. Eng.* 142 (8), 04016037.
- Tian, K., Likos, W.J., Benson, C.H., 2019. Polymer elution and hydraulic conductivity of bentonite-polymer composite geosynthetic clay liners. *J. Geotech. Geoenviron. Eng.* 145 (10), 04019071.
- Tincopa, M., Bouazza, A., Rowe, R.K., Rahardjo, H., 2020. Back-analysis of the water retention curve of a GCL on the wetting path. *Geosynth. Int.* 27 (5), 523–537.
- Tincopa, M., Bouazza, A., 2021. Water retention curves of a geosynthetic clay liner under non-uniform temperature-stress paths. *Geotext. Geomembranes* 49 (5), 1270–1279.
- Touze-Foltz, N., Bannour, H., Barral, C., Stoltz, G., 2016. A review of the performance of geosynthetics for environmental protection. *Geotext. Geomembranes* 44 (5), 656–672.
- Tuller, M., Or, D., 2005. Water films and scaling of soil characteristic curves at low water contents. *Water Resour. Res.* 41 (9).
- Tuller, M., Or, D., Dudley, L.M., 1999. Adsorption and capillary condensation in porous media: liquid retention and interfacial configurations in angular pores. *Water Resour. Res.* 35 (7), 1949–1964.
- Villar, M.V., Lloret, A., 2008. Influence of dry density and water content on the swelling of a compacted bentonite. *Appl. Clay Sci.* 39 (1–2), 38–49.
- Van Genuchten, M.T., 1980. A closed-form equation for predicting the hydraulic conductivity of unsaturated soils. *Soil Sci. Soc. Am. J.* 44 (5), 892–898.
- Villar, M.V., Gómez-Espina, R., Campos, R., Barrios, I., Gutiérrez, L., 2012. Porosity changes due to hydration of compacted bentonite. In: *Unsaturated Soils: Research and Applications*. Springer, Berlin, Heidelberg, pp. 137–144.
- Wireko, C., Zainab, B., Tian, K., Abichou, T., 2020. Effect of specimen preparation on the swell index of bentonite-polymer GCLs. *Geotext. Geomembranes* 48 (6), 875–885.
- Yang, H., Rahardjo, H., Leong, E.C., Fredlund, D.G., 2004. Factors affecting drying and wetting soil-water characteristic curves of sandy soils. *Can. Geotech. J.* 41 (5), 908–920.
- Yesiller, N., Hanson, J.L., Risken, J.L., Benson, C.H., Abichou, T., Darius, J.B., 2019. Hydration fluid and field exposure effects on moisture-suction response of geosynthetic clay liners. *J. Geotech. Geoenviron. Eng.* 145 (4), 04019010.
- Yu, B., El-Zein, A., 2020. Water characteristic curves of geosynthetic clay liners hydrated by a saline solution. *Geosynth. Int.* 1–14.
- Zhang, L., Chen, Q., 2005. Predicting bimodal soil-water characteristic curves. *J. Geotech. Geoenviron. Eng.* 131 (5), 666–670.